Dynamic NMR Study of the Kinetic HH/HD/DD Isotope Effects on the Double Proton Transfer in Cyclic Bis(*p*-fluorophenyl)formamidine Dimers†

Ludger Meschede‡ and Hans-Heinrich Limbach*,§

Institut für Physikalische Chemie der Universität Freiburg i.Br., Albertstrasse 21, D-7800 Freiburg, Germany
(Received: March 8, 1991)

The ^1H and ^{19}F NMR spectra of $^{15}N,^{15}N'$-bis(*p*-fluorophenyl)formamidine (DFFA) dissolved in tetrahydrofuran (THF) were measured and analyzed as a function of temperature, concentration, and deuterium fraction in the mobile proton sites. DFFA exists in THF as an s-trans conformer A and an s-cis conformer B. At low concentrations both conformers are present as monomers A_1 and B_1, which are hydrogen bonded to the solvent. At higher concentrations, A forms cyclic dimers A_2. In these dimers, a double proton transfer takes place characterized by kinetic HH/HD/DD isotope effects. The following thermodynamic and kinetic quantities were obtained by NMR line-shape analysis and magnetization transfer experiments in the rotating frame. The equilibrium constant of the isomerization is given by $K_{B_1A_1} = \exp[(-2 \pm 1 \text{ J mol}^{-1} \text{ K}^{-1})/R] \exp[(1.0 \pm 0.2 \text{ kJ mol}^{-1})/RT]$, 176 K < T < 271 K. The rate constant of the interconversion is given by $k_{A_1B_1} = 10^{14.3\pm1.0} \exp[(-62.5 \pm 1.0 \text{ kJ mol}^{-1})/RT]$ s^{-1}, 237 K < T < 302 K. The equilibrium constant of the formation of A_2 from A_1 is given by

$$K_{A_2} = \exp[(-29 \pm 1 \text{ J mol}^{-1} \text{ K}^{-1})/R] \exp[(5.7 \pm 0.3 \text{ kJ mol}^{-1})/RT] \text{ L mol}^{-1}, \quad 170 \text{ K} < T < 254 \text{ K}$$

For the tautomerism in the cyclic dimer the following isotopic rate constants were obtained: $k_{A_2}^{HH} = 10^{9.9\pm0.3} \exp[(-18.9 \pm 0.3 \text{ kJ mol}^{-1})/RT]$ s^{-1}; $k_{A_2}^{HD} = 10^{10.7\pm0.3} \exp[(-26.7 \pm 0.3 \text{ kJ mol}^{-1})/RT]$ s^{-1}; $k_{A_2}^{DD} = 10^{11.5\pm0.3} \exp[(-33.4 \pm 0.3 \text{ kJ mol}^{-1})/RT]$ s^{-1}, 164.2 K < T < 260.9 K; with the kinetic isotope effects of $k_{A_2}^{HH}/k_{A_2}^{HD} = 23 \pm 4$, $k_{A_2}^{HD}/k_{A_2}^{DD} = 10 \pm 2$, $k_{A_2}^{HH}/k_{A_2}^{DD} = 237 \pm 20$ at 189.2 K. The Arrhenius curves of all isotopic reactions could be simulated in terms of a concerted proton transfer that proceeds by thermally activated tunneling at low temperatures. This result is in contrast to previous findings for intramolecular degenerate double proton transfer reactions where stepwise reaction pathways have been established. With a three-dimensional model potential surface it is shown, however, that the difference between the concerted and the stepwise reaction pathway disappears when the hydrogen bond length is decreased during the course of the reaction. It follows that the observed kinetic isotope effects are in agreement with both a concerted or a stepwise reaction pathway in a compressed hydrogen-bonded state.

Introduction

In 1969 Taylor, El-Bayoumi, and Kasha found evidence of a photoinduced nondegenerate double proton transfer in cyclic 7-azaindole dimers.[1] In subsequent studies[2-11] this process was studied in more detail, especially in supercooled jet streams.[8-11] Thus, it was found that the phototautomerism of 7-azaindole is characterized by kinetic HH/DD isotope effects. It has been argued that proton tunneling must play a role in this reaction[2-9] and that the reaction can be promoted by excitation of the symmetric hydrogen-bonded stretching vibration.[10,11]

To obtain further information on the mechanisms of double proton transfer reactions, the measurement of the full kinetic HH/HD/DD isotope effects is desirable. These effects can be obtained for degenerate or near-degenerate reaction systems by dynamic liquid- and solid-state NMR techniques of suitably isotopically labeled compounds.[12-25] A search for symmetric analogues of 7-azaindole exhibiting similar hydrogen bonding and proton transfer capabilities leads to the class of amidines RNHCH=NR. Evidence for a liquid-state tautomerism of symmetric *N,N'*-diarylamidines has been obtained by Borisov et al.[26] We have recently studied the dynamics of *N,N'*-diphenylformamidine (DPFA) dissolved in tetrahydrofuran by ^1H NMR spectroscopy.[19] For this purpose DPFA had to be labeled with the ^{15}N isotope to avoid ^{14}N quadrupole effects on the NMR spectra. Experiments were performed on the mobile ^1H–^{15}N proton signals at different concentrations and temperatures in the mobile proton sites. Thus, good evidence could be obtained for the reaction network shown in Figure 1. DPFA is subject to a conformational isomerism between an s-trans form A and an s-cis form B. The latter is present as a monomer B_1, hydrogen bonded to the solvent. At low concentrations the s-trans form also forms solvated monomers A_1. However, at higher concentrations A

† Presented at the Conference "Photoinduced Proton Transfer Dynamics in Chemistry, Biology, and Physics" in honor of Professor Michael Kasha, Tallahassee, FL, Jan 6–9, 1991.

‡ Present address: Conti Tech Antriebssysteme GmbH, Forschung und Entwicklung, Philipsbornstr. 1, D-3000 Hannover 1, F.R.G.

§ Present address: Fachbereich Chemie, Institut für Organische Chemie, Takustr. 3, D-1000 Berlin 33, F.R.G.

(1) Taylor, C. A.; El-Bayoumi, M. A.; Kasha, M. *Proc. Nat. Acad. Sci. U.S.A.* **1969**, *63*, 253.
(2) Ingham, K. C.; Abu-Elgheit, M.; El-Bayoumi, M. A. *J. Am. Chem. Soc.* **1971**, *93*, 5023.
(3) Ingham, K. C.; El-Bayoumi, M. A. *J. Am. Chem. Soc.* **1974**, *96*, 1674.
(4) El-Bayoumi, M. A.; Avouris, P.; Ware, W. R. *J. Chem. Phys.* **1975**, *62*, 2499.
(5) Avouris, P.; Yang, L.; Li, L.; El-Bayoumi, M. A. *Photochem. Photobiol.* **1976**, *24*, 211.
(6) Bulska, H.; Chodkowska, A. *J. Am. Chem. Soc.* **1980**, *102*, 3259.
(7) Chang, C.; Shabestary, N.; El-Bayoumi, M. A. *Chem. Phys. Lett.* **1980**, *75*, 107.
(8) Tokumura, K.; Watanabe, Y.; Itoh, M. *J. Phys. Chem.* **1986**, *90*, 2362.
(9) Tokumura, K.; Watanabe, Y.; Udagawa, M.; Itoh, M. *J. Am. Chem. Soc.* **1987**, *109*, 1346.
(10) Fuke, K.; Yabe, T.; Chiba, N.; Kohida, T.; Kaya, K. *J. Phys. Chem.* **1986**, *90*, 2309.
(11) Fuke, K.; Kaya, K. *J. Phys. Chem.* **1986**, *93*, 614.
(12) Limbach, H. H.; Hennig, J.; Gerritzen, G.; Rumpel, H. *Faraday Discuss. Chem. Soc.* **1982**, *74*, 229.
(13) Gerritzen, D.; Limbach, H. H. *Ber. Bunsen-Ges. Phys. Chem.* **1981**, *85*, 527.
(14) Gerritzen, D.; Limbach, H. H. *J. Am. Chem. Soc.* **1984**, *106*, 869.
(15) Schlabach, M.; Wehrle, B.; Limbach, H. H.; Bunnenberg, E.; Knierzinger, A.; Shu, A.; Tolf, B. R.; Djerassi, C. *J. Am. Chem. Soc.* **1986**, *108*, 3856.
(16) Otting, G.; Rumpel, H.; Meschede, L.; Scherer, G.; Limbach, H. H. *Ber. Bunsen-Ges. Phys. Chem.* **1986**, *90*, 1122.
(17) Rumpel, H.; Limbach, H. H. *J. Am. Chem. Soc.* **1989**, *111*, 5429.
(18) Scherer, G.; Limbach, H. H. *J. Am. Chem. Soc.* **1989**, *111*, 5946.
(19) Meschede, L.; Gerritzen, D.; Limbach, H. H. *Ber. Bunsen-Ges. Phys. Chem.* **1988**, *92*, 469.
(20) Meschede, L.; Scherer, G.; Limbach, H. H. *Z. Naturforsch.* **1989**, *44a*, 459.
(21) Limbach, H. H. Dynamic NMR Spectroscopy in the Presence of Kinetic Hydrogen Deuterium Isotope Effects. In *NMR Basic Principles and Progress*; Springer-Verlag: Berlin, 1991; Chapter 2.
(22) Limbach, H. H.; Hennig, J.; Kendrick, R. D.; Yannoni, C. S. *J. Am. Chem. Soc.* **1984**, *106*, 4059.
(23) Limbach, H. H.; Wehrle, B.; Zimmermann, H.; Kendrick, R. D.; Yannoni, C. S. *Angew. Chem., Int. Ed. Engl.* **1987**, *26*, 247.

0022-3654/91/2095-10267$02.50/0

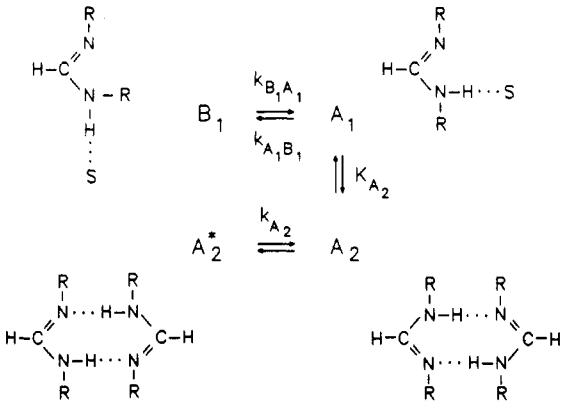

Figure 1. Exchange processes of *N,N'*-diarylamidines in THF as identified by NMR spectroscopy.[19,20] DPFA: R = phenyl. DFFA: R = *p*-fluorophenyl.

forms cyclic dimers A_2. The kinetics of proton exchange between DPFA molecules was followed as a function of concentration and temperature. It was found that A but not B exchanges protons; two molecules were involved in the exchange. ^{1}H NMR experiments at different deuterium fractions in the mobile proton sites allowed us to determine the number of protons transferred in the rate-limiting step to be $m = 2$ and to establish a kinetic HH/HD isotope effect on the exchange. Thus, evidence was obtained that the double proton transfer takes place in the cyclic dimer A_2. Unfortunately, only the kinetic HH/HD isotope effects could be obtained for DPFA because of absence of a suitable spin label sensitive to these effects.

In a recent paper[20] we could, however, show that the full kinetic HH/HD/DD isotope effects on the amidine tautomerism can be obtained by ^{19}F NMR spectroscopy of *N,N'*-bis(*p*-fluorophenyl)formamidine (DFFA). Experiments were reported for one concentration at 189.2 K where the kinetic HH/HD/DD isotope effects were given by the values 233:11:1. This result constitutes a substantial deviation from the so-called "rule of the geometric mean" (RGM), which states that

$$k^{HD} = (k^{HH}k^{DD})^{1/2}, \quad \text{i.e.,} \quad k^{HH}/k^{HD} = k^{HD}/k^{DD} \qquad (1)$$

The RGM has been derived from a combination of transition-state[27] and Bigeleisen's equilibrium isotope effect or isotope fractionation theory[28-34] for the case of a concerted double proton transfer over the barrier. In recent years several cases were found where deviations from the RGM were observed.[12,14,17,18,20,21,35,36] For example, the kinetic HH/HD/DD isotope effects of proton exchange in cyclic 1:1 complexes of acetic acid and methanol dissolved in THF were given by the values 15:3:1 at 298 K.[14] This result could be interpreted in terms of a concerted proton motion involving tunneling. Larger deviations were observed for intramolecular double proton transfer systems.[12,17,18] The kinetic isotope effects of these reactions could be described by the equation

$$\frac{k^{HD}}{k^{DD}} = \frac{2}{S^{-1} + P^{-1}}, \quad \frac{k^{HH}}{k^{DD}} = PS, \quad P \gg S \simeq 1 \qquad (2)$$

derived by using formal kinetics for the case of a stepwise proton transfer mechanism.[17] Here, P represents the primary kinetic H/D isotope effect of the proton in flight and S the secondary isotope effect of the bound proton. Increasing S in eq 2 from the usual value of 1 to P as expected for a concerted double proton transfer leads to eq 1.

Recently, the structure of the transition state of the double proton transfer in formamidine dimers has been studied by using ab initio methods.[37,38] It is very interesting to note that as the level of sophistication in the calculations is increased, a switch from a concerted to a stepwise reaction pathway is observed.

To elucidate experimentally the mechanism of the double proton transfer in formamidine dimers, we herewith report on the results of a systematic study of the system DFFA/THF as a function of temperature, concentration, and deuterium fraction in the mobile proton sites using various methods of dynamic NMR spectroscopy. Thus, the kinetic HH/HD/DD isotope effects on the double proton transfer in cyclic DFFA dimers could be obtained in a wide temperature range. The paper is organized as follows: After an experimental section, we review in a theoretical part the formalism used for deriving the kinetic data from the NMR experiments. Then the experimental results are reported. The discussion deals with the questions as to whether tunneling is involved, whether the reaction is concerted or stepwise, and how compression of the hydrogen bonds may affect the two pathways.

Experimental Section

Synthesis of Isotopically Labeled DFFA. ^{15}N-labeled DFFA was prepared as described previously[20] from ^{15}N-labeled *p*-fluoroaniline. The latter was synthesized from *p*-fluorobenzoic acid and $^{15}NH_4Cl$ via the amide and subsequent Hoffmann degradation.

Sample Preparation. The sealed DFFA NMR samples had to be prepared very carefully on a vacuum line in order to exclude air and moisture and any other impurities that might catalyze the proton exchange. The procedure is similar to that described for DPFA.[19] Since the density of THF is temperature dependent, the concentrations $C(T)$ at temperature T were calculated for each sample using the following equation:[39]

$$C(T)/C(298\ \text{K}) = 1 + 9.26 \times 10^{-4}(298 - T) \qquad (3)$$

The values of C(298 K) and of the deuterium fraction D in the mobile proton site were checked by ^{1}H NMR spectroscopy. A 0.25 M sample was used as a reference.

NMR Measurements. The 300-MHz ^{1}H NMR spectra were recorded with a Bruker MSL 300 pulse FT NMR spectrometer, the 84.7-MHz ^{19}F NMR spectra with a Bruker CXP 100 pulse FT NMR spectrometer working at 90.02 MHz for ^{1}H. During the ^{19}F NMR experiments the protons were decoupled by using the continuous-wave homodecoupling technique, with the irradiating frequency being centered on the aromatic protons. For temperature control a Bruker B VT 100 unit was employed. The sample temperatures were checked before and after each experiment with a Pt 100 resistance thermometer (Degussa) imbedded in an NMR tube; they are estimated to be accurate to about 0.5 °C. The temperature stability during the measurements was, however, better than 0.2 °C. The spectra were transferred from the Bruker minicomputers Aspect 3000/2000 to a personal computer and then to the Univac 1108 computer of the Rechenzentrum der Universität Freiburg. Kinetic and thermodynamic parameters were obtained by simulation of the spectra, as described below. Various experimental data were fitted to theoretical curves by using a nonlinear least-squares fit program.

(24) Wehrle, B.; Limbach, H. H.; Köcher, M.; Ermer, O.; Vogel, E. *Angew. Chem., Int. Ed. Engl.* **1987**, *26*, 934.
(25) Smith, J. A. S.; Wehrle, B.; Aguilar-Parilla, F.; Limbach, H. H.; Foces-Foces, M.; Cano, F. H.; Elguero, J.; Baldy, A.; Pierrot, M.; Khurshid, M. M. T.; Larcombe-McDuall, J. B. *J. Am. Chem. Soc.* **1989**, *111*, 7304.
(26) Borisov, E. V.; Kratsov, D. N.; Peregudov, A. S.; Fedin, E. I. *Izv. Akad. Nauk SSSR, Ser. Khim.* **1980**, *9*, 2151.
(27) Glasstone, S.; Laidler, K. J.; Eyring, H. *The Theory of Rate Processes*; McGraw-Hill: New York, 1941.
(28) Gold, V. *Trans. Faraday Soc.* **1960**, *56*, 255; *Adv. Phys. Org. Chem.* **1969**, *7*, 259.
(29) Albery, W. J. *Prog. React. Kinet.* **1967**, *4*, 355.
(30) Waldmann, L. *Naturwissenschaften* **1943**, *31*, 205.
(31) Bigeleisen, J.; Goeppert-Mayer, M. *J. Chem. Phys.* **1947**, *15*, 261.
(32) Bigeleisen, J. *J. Chem. Phys.* **1955**, *23*, 2264.
(33) Gandour, R. D.; Schowen, R. L. *Transition States of Biochemical Processes*; Plenum Press: New York 1978.
(34) Albery, W. J. *J. Phys. Chem.* **1986**, *90*, 3773.
(35) Ahlberg, P.; Jannê, K.; Löfås, S.; Nettelblad, F.; Swahn, L. *J. Phys. Org. Chem.* **1989**, *2*, 429.
(36) Schlabach, M.; Scherer, G.; Limbach, H. H. *J. Am. Chem. Soc.* **1991**, *113*, 3550.
(37) Svensson, P.; Bergmann, N. Å.; Ahlberg, P. *Z. Naturforsch.* **1989**, *44a*, 473.
(38) Nguyen, K. A.; Gordon, M. S.; Truhlar, D. G., *J. Am. Chem. Soc.* **1991**, *113*, 1596.
(39) Carvajal, C.; Tölle, K. J.; Smid, J.; Swarc, M. *J. Am. Chem. Soc.* **1965**, *87*, 5548. Metz, D. J.; Glines, A. *J. Phys. Chem.* **1967**, *71*, 1158.

Theoretical Section

Evaluation of Kinetic Data from the NMR Spectra of DFFA. (a) Definition of the Kinetic Quantities. Let us first recall the kinetic and thermodynamic quantities that determine the exchange-broadened NMR spectra in the presence of a simple molecular interconversion:

$$i \rightleftharpoons j \tag{4}$$

characterized by the equilibrium constant

$$K_{ij} = k_{ij}/k_{ji} = C_j/C_i \tag{5}$$

C_i is the concentration of species i and k_{ij} the pseudo-first-order rate constant of the interconversion from i to j. NMR experiments are generally performed under equilibrium conditions. The NMR line shapes depend on the inverse lifetimes:

$$\tau_{ij}^{-1} = k_{ij} = -C_i^{-1}\, dC_{i\rightarrow j}/dt \tag{6}$$

$dC_{i\rightarrow j}/dt$ is the number of moles per liter of species i reacting per second to j.

Here we consider the molecules AL, AM*, where L, M* = H, D represent mobile protons and deuterons subject to the following isotopic exchange reactions:

$$\begin{aligned} &AH \xrightarrow{\tau_{AHAH^*}^{-1}} AH^*, \quad AH \xrightarrow{\tau_{AHAD}^{-1}} AD, \\ &AD \xrightarrow{\tau_{ADAH}^{-1}} AH, \quad AD \xrightarrow{\tau_{ADAD^*}^{-1}} AD^*, \end{aligned} \tag{7}$$

$$AH \xrightarrow{\tau_{AHA^*H}^{-1}} A^*H, \quad AD \xrightarrow{\tau_{ADA^*D}^{-1}} A^*D \tag{8}$$

In eqs 7 and 8 asterisks are introduced to characterize physically different but chemically identical particles. $\tau_{ALAL^*}^{-1}$, with LL* = HH, HD, DD, represents the pseudo-first-order exchange rate constant of group A between the environments AL and AL*, i.e., the inverse correlation time of group A with spin L before the latter is replaced by spin L*. $\tau_{ALA^*L}^{-1}$ represents the inverse lifetime of the isotope L before the transfer from A to environment A* takes place. These lifetimes are obtained from eq 6 as follows:

$$\tau_{ALAL^*}^{-1} = -(1/C_{AL})\, dC_{AL\rightarrow AL^*}/dt, \qquad LL = HH, HD, DH, DD$$

$$\tau_{AHA^*H}^{-1} \equiv \tau_{AH}^{-1} = -(1/C_{AH})\, dC_{AH\rightarrow A^*H}/dt \tag{9}$$

$$\tau_{ADA^*D}^{-1} \equiv \tau_{AD}^{-1} = -(1/C_{AD})\, dC_{AD\rightarrow A^*D}/dt$$

It is evident that τ_{ALAL}^{-1} can be determined only by line-shape analysis of the remote A-spin spectra. By contrast, $\tau_{ALA^*L}^{-1}$ is obtained by NMR spectroscopy of the L spins. The different inverse lifetimes in eq 9 can, however, be obtained only if the hydrogen-exchange process to be studied modulates the spin hamiltonian of the A and/or of the mobile isotopes L. As shown in the following, information on the kinetic hydrogen/deuterium isotope effects can be obtained by monitoring the dependence of the correlation times as a function of the deuterium fraction of the sample.

To be more specific, let us consider now the following isotopic double hydrogen transfer reaction set:

$$AH + A^*H^* \xrightarrow{k_2^{HH}} AH^* + A^*H \tag{10}$$

$$AH + A^*D \xrightarrow{k_2^{HD}} AD + A^*H \tag{11}$$

$$AD + A^*D^* \xrightarrow{k_2^{DD}} AD^* + A^*D \tag{12}$$

where k_2^{LL} is the second-order rate constant of the LL reaction. We are interested in a relation between the inverse lifetimes and the k_2^{LL} values. Let

$$C_A = C_{AH} + C_{AD} \tag{13}$$

be the total concentration of A. Using conventional kinetics, we obtain

$$\tau_{AHAH^*}^{-1} = k_2^{HH}C_{AH} = (1 - D)k_2^{HH}C_A = (1 - D)k^{HH} \tag{14}$$

$$\tau_{AHAD}^{-1} = k_2^{HD}C_{AH} = Dk_2^{HD}C_A = Dk^{HD} \tag{15}$$

$$\tau_{ADAH}^{-1} = k_2^{HD}C_{AH} = (1 - D)k_2^{HD}C_A = (1 - D)k^{HD} \tag{16}$$

$$\tau_{ADAD^*}^{-1} = k_2^{DD}C_{AH} = Dk_2^{DD}C_A = Dk^{DD} \tag{17}$$

$$\tau_{AHA^*H}^{-1} = \tau_{AH}^{-1} = k_2^{HH}C_{AH} + k_2^{HD}C_{AD} = ((1 - D)k_2^{HH} + Dk_2^{HD})C_A = (1 - D)k^{HH} + Dk^{HD} \tag{18}$$

$$\tau_{ADA^*D}^{-1} = \tau_{AD}^{-1} = k_2^{HD}C_{AH} + k_2^{DD}C_{AD} = ((1 - D)k_2^{HD} + Dk_2^{DD})C_A = (1 - D)k^{HD} + Dk^{DD} \tag{19}$$

All quantities are linearly dependent on the deuterium fraction D. It is convenient to combine the total concentration C_A with the constants k_2^{LL} to the pseudo-first-order rate constants k^{LL}.

(b) NMR Line-Shape Theory. NMR line shapes are determined by the time evolution of the transverse elements of the density matrix ρ^t during the acquisition time. In the absence of high-order spin–spin coupling, the elements of ρ^t are equal to the expectation values G of the complex transverse magnetization. In the Liouville space the time evolution of ρ^t is given by the master equation

$$d\rho^t/dt = \mathcal{M}^t\rho^t \tag{20}$$

For $t \rightarrow \infty$ the elements of ρ^t vanish, i.e., $\rho^t(\infty) = 0$. If the elements of ρ^t at $t = 0$ and $\mathcal{M}$ are known, eq 20 can be solved and the line shapes calculated by using known procedures.[40,41] The matrix $\mathcal{M}^t$ depends on whether experiments are performed on the mobile hydrogen isotopes L = H, D or on remote spins in the remaining group A. In the case of DFFA the chemical shift of the exchanging proton is not modulated during the exchange. Therefore, the line shapes of the latter are sensitive to the exchange only if the scalar spin–spin interaction to spins in A is modulated. This is the case when the nitrogen atoms in DFFA are labeled with the ^{15}N isotope. The line-shape theory for this case has been described.[19,21] Basically, from the line-shape analysis of the labile proton the quantity $\tau_{AHXH}^{-1} = \tau_{AH}^{-1}$ can be derived which, for a double proton transfer, depends on the pseudo-first-order rate constants k^{HH} and k^{HD} according to eq 18.

Within the context of this study, NMR experiments have been performed mainly on the remote ^{19}F spins in the remaining group A. In this case, both species AH and AD contribute to the line shape of A. Let us consider here the simplest case, where high-order scalar spin–spin coupling between A spins and L spins can be neglected and where the chemical shift of A is modulated by the exchange. Then, eq 20 can be replaced by a similar equation of the complex transverse magnetizations G. Let ν_{AL} be the chemical shift of A before and $\nu_{A'L}$ the chemical shift after the exchange. The time dependence of the elements of G that determine the line shape can then be described by eq 21, Chart I, where for one-pulse experiments $\rho^t(0)$ is given by the population vector

$$P = [p_{AH};p_{A'H};p_{AD};p_{A'D}], \quad \text{with } \tau_{AHAD}^{-1}/\tau_{ADAH}^{-1} = p_{AD}/p_{AH} \tag{22}$$

$T_2 = 1/(\pi W_0)$ is the effective transverse relaxation time, and W_0 the line width in the absence of exchange. For the case of a double proton transfer eq 23 (Chart II) follows from eq 14–19, 21, and 22. When the data are collected in one-pulse experiments, the magnetizations at $t = 0$ are equal to the elements of the population vector, i.e., given by

$$p_{AH} = p_{A'H} = 1 - D, \quad p_{AD} = p_{A'D} = D \tag{24}$$

(c) Magnetization Transfer in the Rotating Frame. In the slow-exchange range NMR line-shape analysis is not precise enough in order to measure the kinetic quantities. The latter can, however, be obtained in this range by following the time evolution of the magnetizations G in the rotating frame under spin locking conditions.[21,42,43] The time dependence of G is obtained from eq

(40) Binsch, G. *J. Am. Chem. Soc.* **1969**, *91*, 1304.
(41) Ernst, R. R.; Bodenhausen, G.; Wokaun, A. *Principles of Nuclear Magnetic Resonance in One and Two Dimensions*, Clarendon Press: Oxford, 1987.
(42) Hennig, J.; Limbach, H. H. *J. Magn. Reson.* **1982**, *49*, 322.

CHART I

$$\frac{d}{dt}\begin{bmatrix} G_{AH} \\ G_{A'H} \\ G_{AD} \\ G_{A'D} \end{bmatrix} = \begin{bmatrix} -\tau_{AHAH^*}^{-1} - \tau_{AHAD}^{-1} - 1/T_2 + 2\pi i\nu_{AH} & \tau_{AHAH^*}^{-1} & & \tau_{ADAH}^{-1} \\ \tau_{AHAH^*}^{-1} & \tau_{AHAH^*}^{-1} - \tau_{AHAD}^{-1} - 1/T_2 + 2\pi i\nu_{A'H} & \tau_{AHAD}^{-1} & \\ & \tau_{ADAH}^{-1} & -\tau_{ADAH}^{-1} - \tau_{ADAD^*}^{-1} - 1/T_2 + 2\pi i\nu_{AD} & \tau_{ADAD^*}^{-1} \\ \tau_{AHAD}^{-1} & & \tau_{ADAD^*}^{-1} & -\tau_{ADAH}^{-1} - \tau_{ADAD^*}^{-1} - 1/T_2 + 2\pi i\nu_{A'D} \end{bmatrix} \begin{bmatrix} G_{AH} \\ G_{A'H} \\ G_{AD} \\ G_{A'D} \end{bmatrix} \quad (21)$$

CHART II

$$\frac{d}{dt}\begin{bmatrix} G_{AH} \\ G_{A'H} \\ G_{AD} \\ G_{A'D} \end{bmatrix} = \begin{bmatrix} -(1-D)k^{HH} - Dk^{HD} - 1/T_2 + 2\pi i\nu_{AH} & (1-D)k^{HH} & & (1-D)k^{HD} \\ (1-D)k^{HH} & -(1-D)k^{HH} - Dk^{HD} - 1/T_2 + 2\pi i\nu_{A'H} & (1-D)k^{HD} & \\ & Dk^{HD} & -(1-D)k^{HD} - Dk^{DD} - 1/T_2 + 2\pi i\nu_{AD} & Dk^{DD} \\ Dk^{HD} & & Dk^{DD} & -(1-D)k^{HD} - Dk^{DD} - 1/T_2 + 2\pi i\nu_{A'D} \end{bmatrix} \begin{bmatrix} G_{AH} \\ G_{A'H} \\ G_{AD} \\ G_{A'D} \end{bmatrix} \quad (23)$$

21 or 23 by setting all chemical shifts $\nu_i = 0$ and replacing the transverse relaxation time T_2 by the longitudinal relaxation time in the rotating frame, $T_{1\rho}$. The resulting equations can be solved numerically. In the case treated here the symmetry of the exchange matrix can be used in order to reduce the dimensionality of the exchange problem. Thus, we obtain

$$\frac{d}{dt}\begin{bmatrix} G_{AH} + G_{A'H} \\ G_{AD} + G_{A'D} \end{bmatrix} = \begin{bmatrix} -1/T_{1\rho} - \tau_{AHAD}^{-1} & \tau_{ADAH}^{-1} \\ \tau_{AHAD}^{-1} & -1/T_{1\rho} - \tau_{ADAH}^{-1} \end{bmatrix} \begin{bmatrix} G_{AH} + G_{A'H} \\ G_{AD} + G_{A'D} \end{bmatrix} \quad (25)$$

$$\frac{d}{dt}\begin{bmatrix} G_{AH} - G_{A'H} \\ G_{AD} - G_{A'D} \end{bmatrix} = \begin{bmatrix} -1/T_{1\rho} - 2\tau_{AHAH^*}^{-1} - \tau_{AHAD}^{-1} & \tau_{ADAH}^{-1} \\ \tau_{AHAD}^{-1} & -1/T_{1\rho} - 2\tau_{ADAD^*}^{-1} - \tau_{ADAH}^{-1} \end{bmatrix} \times \begin{bmatrix} G_{AH} - G_{A'H} \\ G_{AD} - G_{A'D} \end{bmatrix} \quad (26)$$

These equations are of the type

$$\frac{d}{dt}\begin{bmatrix} I_1 \\ I_2 \end{bmatrix} = \begin{bmatrix} A_{11}A_{12} \\ A_{21}A_{22} \end{bmatrix} \begin{bmatrix} I_1 \\ I_2 \end{bmatrix} \quad (27)$$

whose solutions are given by

$$\begin{bmatrix} I_1(t) \\ I_2(t) \end{bmatrix} = \begin{bmatrix} I_{1+} \\ I_{2+} \end{bmatrix} \exp(\Lambda_+ t) + \begin{bmatrix} I_{1-} \\ I_{2-} \end{bmatrix} \exp(\Lambda_- t) \quad (28)$$

with

$$\Lambda_\pm = \tfrac{1}{2}(A_{11} + A_{22}) \pm \tfrac{1}{2}[(A_{11} - A_{22})^2 + 4A_{12}A_{21}]^{1/2} \quad (29)$$

$$\begin{bmatrix} I_{1\pm} \\ I_{2\pm} \end{bmatrix} = \begin{bmatrix} [\pm A_{12}I_2(0) \pm (A_{11} - \Lambda_\mp)I_1(0)]/(\Lambda_+ - \Lambda_-) \\ [\pm A_{21}I_1(0) \pm (A_{22} - \Lambda_\mp)I_2(0)]/(\Lambda_+ - \Lambda_-) \end{bmatrix} \quad (30)$$

Using the initial values

$$G_{AH}(0) = G_{A'H}(0) = 1 - D, \quad G_{AD}(0) = G_{A'D}(0) = D \quad (31)$$

it can easily be shown that the time evolution of the sums $G_{AH} + G_{A'H}$ and $G_{AD} + G_{A'D}$ are simple exponentials governed by the relaxation time $T_{1\rho}$:

$$G_{AH} + G_{A'H} = 2(1 - D)\exp(-t/T_{1\rho}), \qquad G_{AD} + G_{A'D} = 2D\exp(-t/T_{1\rho}) \quad (32)$$

By contrast, the differences $G_{AH} - G_{A'H}$ and $G_{AD} - G_{A'D}$ are double exponentials. Of special importance are experiments in which

$$G_{AH}(0) = -G_{A'H}(0) = 1 - D, \quad G_{AD}(0) = -G_{AD}(0) = D \quad (33)$$

In the case of large kinetic hydrogen/deuterium isotope effects where

$$\tau_{AHAH^*}^{-1} \gg \tau_{AHAD}^{-1}, \tau_{ADAH}^{-1}, \tau_{ADAD^*}^{-1} \quad (34)$$

we again obtain expressions that are single exponentials:

$$G_{AH} - G_{A'H} = 2(1 - D)\exp[-t(1/T_{1\rho} + 2\tau_{AHAH^*}^{-1} + \tau_{AHAD}^{-1})] \quad (35)$$

$$G_{AD} - G_{A'D} = 2D\exp[-t(1/T_{1\rho} + 2\tau_{ADAD^*}^{-1} + \tau_{ADAH}^{-1})] \quad (36)$$

These equations also follow directly from eq 26 by neglecting the off-diagonal elements. For a double proton transfer reaction it follows with eqs 14–19 that

$$G_{AH} - G_{A'H} = 2(1 - D)\exp[-t(1/T_{1\rho} + 2(1 - D)k^{HH} + Dk^{HD})] \quad (37)$$

$$G_{AD} - G_{A'D} = 2D\exp[-t(1/T_{1\rho} + 2Dk^{DD} + (1 - D)k^{HD})] \quad (38)$$

Equation 38 will be used in the analysis of the deuteron transfer rates of DFFA in the results section.

(d) Effect of Rotational Isomerism on the NMR Line Shapes of DFFA. As shown below, DFFA exists in two conformational states, AL and BL, L = H, D. Only AL is subject to proton transfer. Since no equilibrium and kinetic isotope effects on the conformational isomerism were observed, the rate and equilibrium constants of the latter process are given by

$$K_{AB} = k_{AB}/k_{BA} \quad (39)$$

To describe the exchange-broadened NMR line shapes in the presence of rotational isomerism, eq 21 has to be expanded. Actually, a second diagonal block of dimension 4 has to be added for BL where all proton and deuteron transfer rates are set to zero. The upper (lower) nondiagonal block of the matrix $\mathcal{M}$ contains in its diagonal part the elements k_{AB} (k_{BA}). The latter quantities are substracted from the diagonal elements in such a way that

(43) Limbach, H. H.; Wehrle, B.; Schlabach, M.; Kendrick, R. D.; Yannoni, C. S. *J. Magn. Reson.* **1988**, *77*, 84.

the sum of all elements in each column vanishes.

Evaluation of Concentration-Dependent Kinetic and Thermodynamic Quantities of the DFFA Network. In this section relations between quantities defined in the previous section, obtainable by NMR and the kinetic quantities characterizing the full reaction network of Figure 1, are derived.

(a) Concentration Dependence of the s-cis/s-trans Isomerism. The total concentration C of DFFA is the sum of the concentrations of the conformers A and B:

$$C = C_A + C_B \tag{40}$$

Let c_{A_1} and c_{B_1} the concentrations of the monomers, c_{A_2} the concentration of the cyclic dimer of A. Then

$$C_A = c_{A_1} + 2c_{A_2}, \quad C_B = c_{B_1} \tag{41}$$

Experimentally, the intensity ratio I of both conformers is accessible by signal integration. I is equal to the effective equilibrium constant K_{AB} of the isomerism:

$$I = C_A/C_B = k_{BA}/k_{AB} = K_{BA} \tag{42}$$

I, k_{AB}, and k_{BA} are obtained by line-shape analysis as mentioned in previous section. In Figure 1 it is assumed that the interconversion of A and B takes place only in the quasi-monomeric state. Therefore, K_{AB}, k_{AB}, and k_{BA} are not true constants in contrast to the quantities defined as follows:

$$I_0 = I(C\rightarrow 0) = c_{A_1}/c_{B_1} = K_{B_1A_1} = k_{B_1A_1}/k_{A_1B_1} \tag{43}$$

$$k_{A_1B_1} = -1/c_{A_1}(dc_{A_1\rightarrow B_1}/dt) \tag{44}$$

It follows that

$$k_{AB} = -1/C_A(dC_{A\rightarrow B}/dt) = -1/C_A(dc_{A_1\rightarrow B_1}/dt) = (c_{A_1}/C_A)k_{A_1B_1} \tag{45}$$

By combination of eqs 40 and 42 it follows with $c_{B_1} = C_B$ that

$$C_A = CI/(I + 1) \tag{46}$$

and that

$$c_{A_1} = CI_0/(I + 1) \tag{47}$$

With eq 45 it follows then that

$$k_{AB} = k_{A_1B_1}(I_0/I) \tag{48}$$

For $C \rightarrow 0$, i.e., $I = I_0$, it follows that $k_{AB} = k_{A_1B_1}$. For $C \rightarrow \infty$, $C_A \gg C_B$, $I \rightarrow \infty$ and $k_{AB} = 0$.

Let us now introduce the equilibrium constant K_{A_2} of the dimerization of A:

$$K_{A_2} = c_{A_2}/c_{A_1}^2 \tag{49}$$

By combination of eqs 40, 41, 43, and 49 it follows that

$$C = C_B + C_A = c_{A_1}(1 + 1/I_0) + 2K_{A_2}c_{A_1}^2 \tag{50}$$

$$I = \tfrac{1}{2}[I_0 - 1 + [(1 + I_0)^2 + 8K_{A_2}CI_0^2]^{1/2}] \tag{51}$$

$$C = \tfrac{1}{2}[(I + 1)(I - I_0)/K_{A_2}I_0^2] \tag{52}$$

Thus, by measuring I as a function of C, one can obtain the equilibrium constant K_{A_2} of the dimerization of A.

(b) Concentration Dependence of Chemical Shifts. Information about K_{A_2} can also be obtained from the analysis of the chemical shifts of A. Since the quasimonomers and the dimers are in fast exchange, the average chemical shift of any nucleus in A is given by

$$\nu_A = \nu_{A_1}c_{A_1}/C_A + 2\nu_{A_2}c_{A_2}/C_A \tag{53}$$

By simple arithmetic using eqs 41, 49, and 53 it follows that[19]

$$\nu_A = \nu_{A_1} + (\nu_{A_2} - \nu_{A_1})\left[1 - \frac{1}{4K_{A_2}C_A}[(8K_{A_2}C_A + 1)^{1/2} - 1]\right] \tag{54}$$

For $C_A \rightarrow 0$, $\nu_A = \nu_{A_1}$ and for $C_A \rightarrow \infty$, $\nu_A = \nu_{A_2}$.

(c) Concentration Dependence of the Proton Exchange Rates. The rate law of proton exchange between the s-trans conformers of DFFA dissolved in THF is complicated by the dimerization step in Figure 1, which precedes the proton exchange. The following expression for the concentration dependence of the pseudo-first-order rate constants k has been derived:[19,21]

$$k = k_{A_2}\frac{4K_{A_2}C_A - (8K_{A_2}C_A + 1)^{1/2} + 1}{4K_{A_2}C_A + (8K_{A_2}C_A + 1)^{1/2} - 1} \tag{55}$$

Thus, k is a nonlinear function of C_A. For small values of C_A it follows from eq 55 that $k = K_{A_2}k_{A_2}C_A$, i.e., a second-order rate law because all molecules are present as monomers. For large values of C_A all molecules are present as cyclic dimers in which the exchange takes place. Then, $k = k_{A_2}$, i.e., k is independent of concentration. In other words, the rate law is of first order. For the special case of the network in Figure 1 the following expression can be derived:[19]

$$k = k_{A_2}(I - I_0)(I + I_0) = k_{A_2}\frac{[(1 + I_0)^2 + 8K_{A_2}C + I_0^2]^{1/2} - I_0 - 1}{[(1 + I_0)^2 + 8K_{A_2}C + I_0^2]^{1/2} + 3I_0 - 1} \tag{56}$$

Thus, k is a linear function of the experimental quantity $(I - I_0)(I + I_0)$. From the slope the rate constant k_{A_2} can be obtained.

In the absence of equilibrium isotope effects on the dimerization step $(I - I_0)(I + I_0)$ is independent of the deuterium fraction in the mobile proton sites. Then, the kinetic isotope effects on k_{A_2} and on k are the same. For this case the simple equation has been derived:[19]

$$\tau_{AH}^{-1}(C\rightarrow\infty,D)/\tau_{AH}^{-1}(C\rightarrow\infty,D=0) = 1 - (1 - k_{A_2}^{HD}/k_{A_2}^{HH})D \tag{57}$$

Results

In this section we first describe the ^1H and ^{19}F NMR experiments performed on DFFA dissolved in tetrahydrofuran as a function of concentration, the deuterium fraction in the mobile proton sites, and temperature. Then kinetic and thermodynamic parameters are derived either by line-shape analysis from the spectra or from separate magnetization transfer experiments in the rotating frame. The kinetic data are then analyzed in terms of the reaction network of Figure 1. Thus, equilibrium and rate constants of the s-cis/s-trans isomerism of DFFA, the equilibrium constants of the formation of the cyclic s-trans dimer, the rate law of proton exchange in the dimer including the number of protons transferred, and the double proton transfer rates in the dimer including the kinetic HH/HD/DD isotope effects as a function of temperature are obtained. All numerical data obtained are assembled in Tables 1 to 6, available as supplementary material (see paragraph at end of paper).

Description of the ^1H NMR Experiments. The results of the ^1H NMR experiments are similar to those described previously for DPFA. In the following we will refer to the atom numbering shown in Figure 2. Let us first discuss the 300.13-MHz ^1H NMR spectra of DFFA as a function of the deuterium fraction D in the mobile proton sites. The spectra recorded at a temperature of 189.2 K and a total DFFA concentration of $C_{298K} = 0.02$ mol L^{-1} are shown in Figure 3. As DFFA was labeled with ^{15}N, the signals of the labile protons should be split into ^1H–^{15}N doublets in the absence of intermolecular proton exchange, characterized by the coupling constant J_{ab}. Each doublet line should further be split by coupling with the C–H proton c and the second ^{15}N atom d. Figure 3 shows that this case is realized for signal B_a of the mobile proton a in the s-cis form BH. Since $J_{ac} \simeq J_{ad}$ each doublet line exhibits an effective triplet splitting. By contrast, fast proton exchange should modulate the Larmor frequencies of the mobile proton, which eventually leads to a collapse of the multiplet into a singlet. This is what is observed for signal A_a arising from the mobile proton in the s-trans form AH. Thus, conformer B is not able to exchange protons, in contrast to conformer A. The ^1H–^{15}N signal of the latter evolves from an exchange broadened singlet at $D = 0$ to an exchange-broadened doublet at $D = 0.9$. This observation signifies that the proton exchange between A molecules is already fast at $D = 0$ but slows

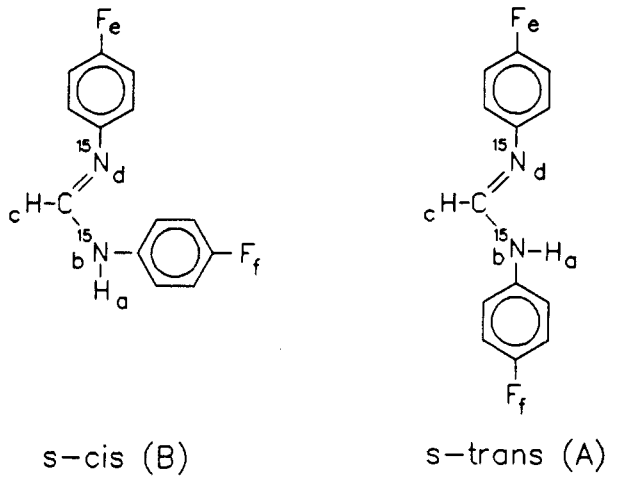

Figure 2. Atom numbering of DFFA in the s-cis and the s-trans forms.

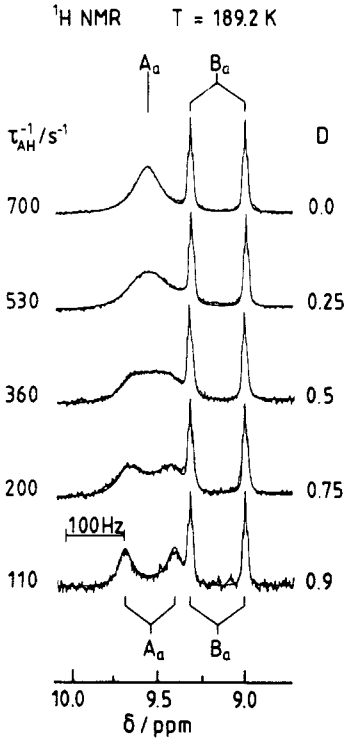

Figure 3. Superposed experimental and calculated 300.13-MHz $^1H-^{15}N$ signals of a 0.02 M solution of DFFA at 189.2 K as a function of the deuterium fraction D in the $^1H-^{15}N$ position. The $^1H-^{15}N$ signals of the s-trans form A are labeled as A_a and of the s-cis form B as B_a in accordance with Figure 2. $\tau_{AH}^{-1} \equiv \tau_{AHAH^*}^{-1}$ is the inverse proton lifetimes in A. Reproduced with permission from ref 20.

down when the deuterium fraction is increased. Therefore, the lifetime $\tau_{AHA^*H} \equiv \tau_{AH}$ of a proton in a given molecule AH before the jump to a chemical equivalent but physically different group A* depends on whether the surrounding molecules in the sample that participate in the exchange are protonated or deuterated. This is the first indication that AH is involved in a multiple proton transfer process and that there is a kinetic HH/HD isotope effect on the reaction. The fact that the signal positions in Figure 3 are constant within the margin of error indicates that both temperature and concentration constancy has been achieved in the set of spectra in Figure 3.

The values of τ_{AH}^{-1} were obtained by line-shape analysis of signal A_a as described in the Theoretical Section. The line widths W_0 in the absence of exchange were obtained by simulation of signal B_a.

The effect of concentration on the spectra of DFFA is shown in Figure 4, for a temperature of 194.5 K. We observe again the same splitting pattern for signal B_a as in Figure 3. The position of B_a is almost independent on concentration. Signal A_c of the

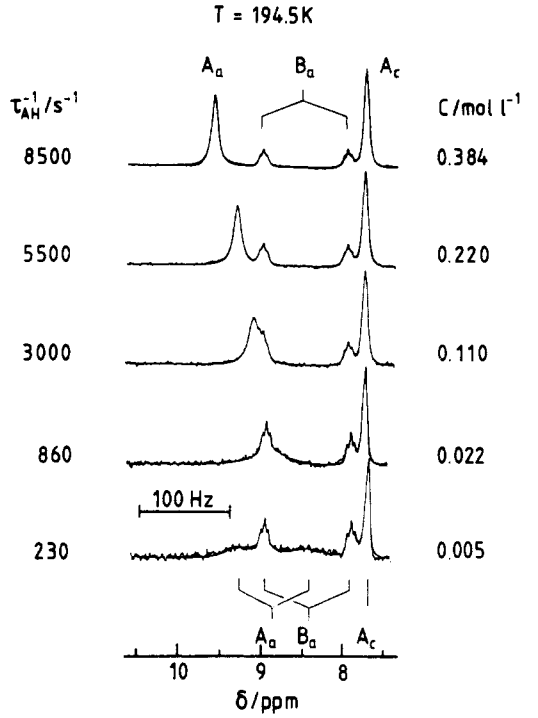

Figure 4. Superposed experimental and calculated 90.02-MHz ^1H NMR spectra of DFFA dissolved in THF as a function of the total concentration C at 194.5 K. A_a, B_a: $^1H-^{15}N$ signals of the conformers A and B. A_c: CH signal of A.

CH protons appears on the high-field side. It does not show any significant changes with concentration. At low concentrations, signal A_a is split into an exchange-broadened doublet. As concentration increases, the components of signal A_a rapidly coalesce into a sharp singlet whereas the components of B_a remain sharp. Signal A_a shifts strongly to low field as concentration is increased by contrast to signal B_a. This is because AH forms cyclic dimers at higher concentrations by contrast to BH. At low concentrations both molecules are quasi-monomers forming a hydrogen bond to the solvent. There is also a small amount of true monomers that induces a shift of A_a and B_a to high field as the temperature is increased. Note that the A-to-B ratio I strongly increases as concentration increases. This effect is also a consequence of the dimerization of AH but not of BH. Note also that the values of $\tau_{AH}^{-1} > 2000\ s^{-1}$ are affected by a large systematic error.

Description of the ^{19}F NMR Experiments. (a) ^{19}F NMR Spectra as a Function of Temperature. Let us first discuss the effect of temperature on the proton-decoupled 84.7-MHz ^{19}F NMR spectra of a 0.35 M sample of DFFA in THF with a deuterium fraction of $D = 0.99$ in the mobile proton sites (Figure 5). The spectrum at 164.3 K shows between 2 and 3.3 ppm four singlets. The s-cis form B contributes the singlets $B_e \equiv BD_e$ and $B_f \equiv BD_f$ to the spectrum, the s-trans form A signals AD_e and AD_f. The subscripts e and f refer to the atom numbering in A and B according to Figure 2. B_e and B_f are of equal intensity. The same is true for A_e and A_f. The s-cis/s-trans ratio I is obtained by line-shape analysis of the signals. Signals AD_e and AD_f are slightly broadened as compared to B_e and B_f. As the temperature is increased, the latter show extensive line broadening due to deuteron exchange between AD molecules in the cyclic dimer. Above 240 K B_e and B_f also show line broadening due to exchange with A_e and A_f via rotational isomerism. At room temperature only one singlet survives due to fast isomerism and deuteron exchange.

The spectra in Figure 5 were calculated as described in the theoretical section. By line-shape analysis one obtains the pseudo-first-order rate constants k_{AB} of the rotational isomerism and the inverse lifetimes $\tau_{ADAD^*}^{-1}$ of the deuteron transfer between the s-trans isomers. Below 240 K the line widths W_0 in the absence of exchange were taken from the signals of the s-cis form B. For the simulations at higher temperatures the W_0 values were extrapolated from low temperature. Below coalescence points,

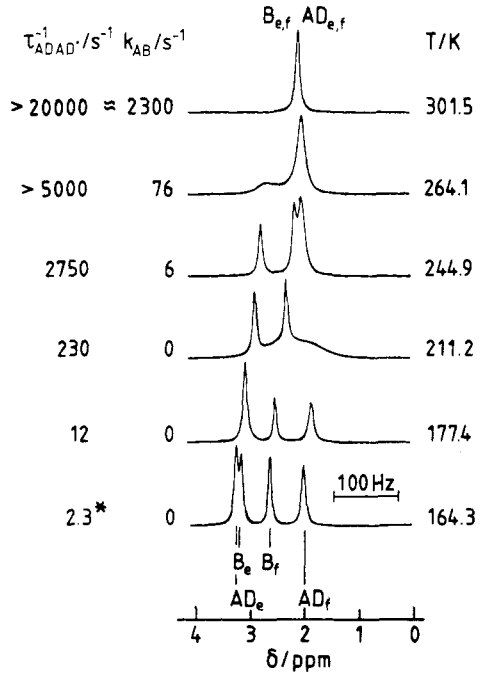

Figure 5. Superposed experimental and calculated 84.7-MHz $^{19}F\{^1H\}$ NMR spectra of a 0.35 M sample of DFFA in THF at a deuterium fraction $D = 0.99$ in the mobile proton sites as a function of temperature. $B_e \equiv BD_e$, $B_f \equiv BD_f$: signals of the s-cis conformer B. AD_e, AD_f: signals of the s-trans conformer A. k_{AB}: pseudo-first-order rate constant of the hindered rotation between the two conformers. $\tau_{ADAD^*}^{-1}$: inverse average lifetime of AD before D is replaced by another D.

chemical shift differences between exchanging lines were directly obtained from the spectra; above the coalescence points these quantities were extrapolated from the low temperature spectra. At low temperature the $\tau_{ADAD^*}^{-1}$ values were obtained via magnetization transfer experiments as described below.

(b) ^{19}F NMR Spectra as a Function of the Deuterium Fraction and Concentration. To obtain full kinetic HH/HD/DD isotope effects of the DFFA proton exchange, ^{19}F NMR experiments were obtained as a function of the deuterium fraction D in the mobile proton sites and of concentration C. Some typical results are shown in Figure 6 for a temperature of 189.2 K. The major difference between the ^1H and the ^{19}F NMR spectra is that in the former only the protonated A and B molecules AH and BH are observed, whereas both A = {AH,AD} and B = {BH,BD} contribute to the ^{19}F NMR spectra. Let us first discuss the spectra at $C = 0.02$ mol L^{-1}. The signals B_e and B_f are not affected by changing the deuterium fraction D in the mobile proton sites. By contrast, the signals of the fluorine atoms of A strongly depend on D. At $D = 0.99$ the signals AD_e and AD_f are sharp, which indicates that the deuteron exchange between the fully deuterated molecules AD is slow. By contrast, at $D = 0$ one broadened coalesced fluorine signal AE_e, AH_f is observed, indicating that a fast proton transfer takes place between the protonated AH molecules. Now, a very interesting phenomenon is observed at intermediate deuterium fractions: the fluorine atoms of the protonated AH and the deuterated AD molecules can be separated, giving rise to a line trio. Whereas the outer two singlets of the trio stem from the AD_e and AD_f, the inner broad line stems from the AH_e, AH_f fluorine atoms. As D is increased, the latter signal becomes broader indicating longer lifetimes of the mobile proton in AH. By contrast, the deuteron lifetime in the deuterated AD molecules shortens as D decreases, leading to a broadening of the outer two singlets. Note that the line intensities AH_e and AH_f are proportional to $(1 - D)/2$, whereas the line intensities AD_e and AD_f are given by $D/2$.

Let us discuss now the effect of increasing concentration on the ^{19}F NMR line shapes of DFFA. As C is increased, the signals AD_e and AD_f at $D = 0.99$ broaden but do not coalesce. At $D = 0$ the coalesced AH_e/AH_f signal sharpens. At 0.35 mol L^{-1} and $D = 0$ the latter becomes sharp because the proton exchange

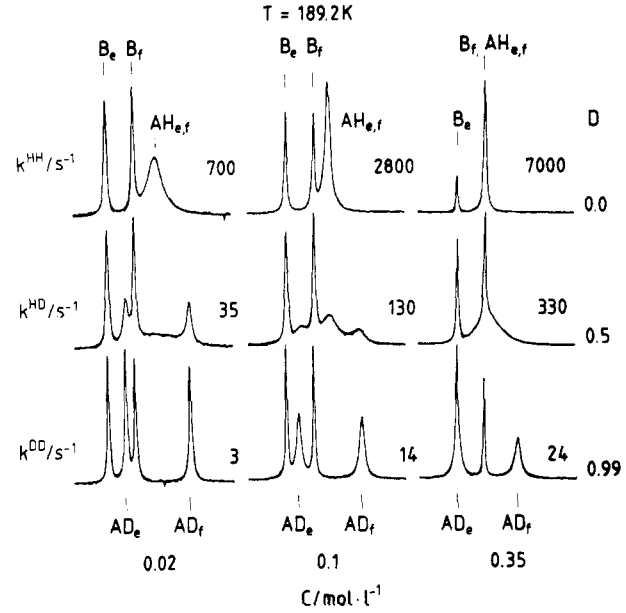

Figure 6. The 84.7-MHz $^{19}F\{^1H\}$ NMR spectra of DFFA in THF as a function of the deuterium fraction D in the mobile proton sites for different total concentrations C at 189.2 K. B_e, $B_f \equiv$ non-exchange-broadened signals of the s-cis form. AL_e, AL_f, L = H, D: signals of the s-trans form A. For further description see text.

is very fast within the NMR time scale. At $D = 0.5$ and $C = 0.02$ mol L^{-1} both the coalesced broad signal $AH_{e,f}$ as well as the slightly broadened separate signals AD_e and AD_f are observable. As C is increased, first $AH_{e,f}$ sharpens whereas AD_e and AD_f broaden; eventually, all signals coalesce.

The spectra in Figure 6 could easily be simulated by using eq 23 where the dynamic parameters are the pseudo-first-order rate constants k^{HH}, k^{HD}, and k^{DD} and by setting $\nu_{AL} = \nu_{AL_e}$ and $\nu_{A'L} = \nu_{AL_f}$.

(c) ^{19}F NMR Magnetization Transfer in the Rotating Frame. Since the signals AD_e and AD_f do not show significant line-broadening, magnetization transfer experiments in the rotating frame were performed on the latter. Two typical sets of experiments carried out at $T = 164.3$ K at deuterium fractions of $D = 0.99$ and $D = 0.5$ are shown in Figure 7. In each case two types of experiments were performed. The data analysis is shown in Figure 8. In experiment i the magnetizations of the lines AD_e and AD_f are parallel, and in experiment ii antiparallel. The decay of AD_e and AD_f in experiment i depends only on the longitudinal relaxation times in the rotating frame, $T_{1\rho}$. In experiment ii the decay of these magnetizations also depends on the deuteron transfer rates τ_{ADAH}^{-1} and $\tau_{ADAD^*}^{-1}$. Since $\tau_{ADAH}^{-1} \gg \tau_{ADAD^*}^{-1}$ the magnetizations in experiment ii decay faster when the deuterium fraction is increased. Further magnetization transfer experiments were performed at different temperatures and concentrations.

Data Analysis. From the experiments described above a wealth of thermodynamic and kinetic parameters arise that are analyzed in this section in terms of the reaction network of Figure 1. We first analyzed the thermodynamic and then the kinetic data.

(a) s-Trans/s-Cis Isomerism and Self-Association of DFFA in THF. The equilibrium constants $K_{B_1A_1}$ of the s-trans/s-cis isomerism between the quasi-monomers $A_1 \equiv AH\cdots S$ and $B_1 \equiv BH\cdots S$, where S is the solvent (Figure 1) were determined from samples with a total concentration of $C(298\text{ K}) = 0.02$ mol L^{-1}. In this range both the A and the B conformer exist as quasi-monomers and the self-association of A can be neglected. In this case the s-trans/s-cis ratio $I = I_0 = K_{B_1A_1}$, according to eq 43. No equilibrium isotope effects on the isomerism could be observed. The data are assembled in Table 3 of the supplementary material. We obtain a reaction entropy and a reaction enthalpy of

$$\Delta S_{A_1B_1} = -2 \pm 1 \text{ J mol}^{-1} \text{ K}^{-1}, \quad \Delta H_{A_1B_1} = 1.0 \pm 0.2 \text{ kJ mol}^{-1} \tag{58}$$

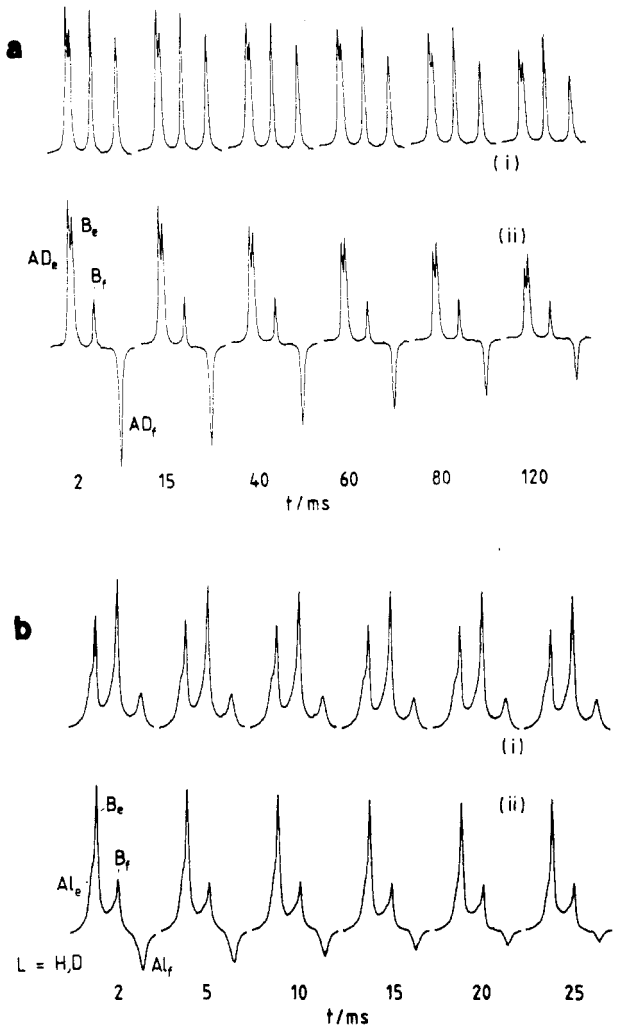

Figure 7. (a) ^{19}F magnetization transfer experiments in the rotating frame performed on a 0.35 M solution of DFFA in THF at 164.3 K and a deuterium fraction $D = 0.99$ in the mobile proton sites. The carrier frequency was set to the position of the AD_f line. Upper curves: experiment i corresponding to a usual $T_{1\rho}$ experiments. Lower curves: experiment ii with a delay $\tau = 1/(2\Delta\nu) = 4.2$ ms between the first 90° pulse and the spin locking pulse. $\Delta\nu$ is the frequency difference between the signals AD_e and AD_f. B_e, B_f: nonexchanging, AD_e, AD_f: exchanging magnetizations. Repetition time 3.8 s, 4.2 μs 90° pulses, strength of the spin locking field $t_{180°} = 165$ μs. (b) Experiments performed under the same conditions as in Figure 7a on a sample with $D = 0.5$.

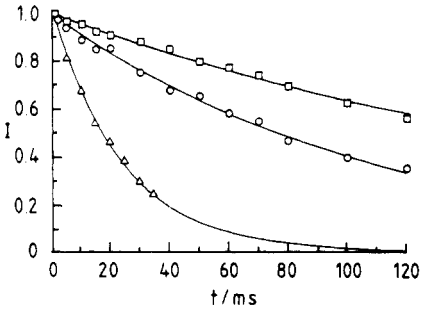

Figure 8. Nonlinear least-squares fit of the data of Figure 7. Upper curve: experiment i at $D = 0.99$; the results at $D = 0.5$ are reproduced by the same curve. Middle curve: experiment ii at $D = 0.99$. Lower curve: experiment ii at $D = 0.5$. The upper curve was analyzed in terms of eq 32, the two lower curves using eq 36.

The equilibrium constants K_{A_2} of the formation of the cyclic dimer A_2 (Figure 1) association were determined in two independent ways. First, the experimental ratios $I = C_A/C_B$ were analyzed as a function of the total concentration C. The dependence $I = f(C)$ could be described in terms of eq 51. The value of I and $C \rightarrow 0$ is equal to the equilibrium constant $I_0 = K_{B_1A_1}$

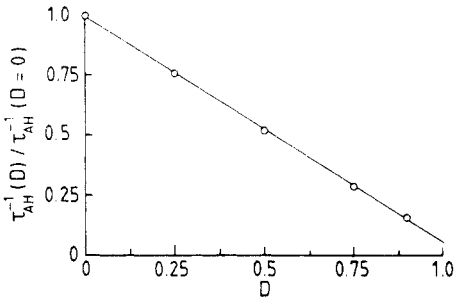

Figure 9. ^1H NMR proton inventory plot of the data in Figure 3. In accordance with eq 57, a linear dependence $\tau_{AH}^{-1} = f(D)$ is expected for a double proton transfer process. The ratio $\tau_{AH}^{-1}(D=0)/\tau_{AH}^{-1}(D=1)$ represents the kinetic HH/HD isotope effect of the exchange.

defined in Figure 1 and eq 43; the nonlinearity of the curves $I = f(C)$ is determined by K_{A_2}. By nonlinear least-squares fitting, we find at 194.5 K a value of $K_{A_2} = 1.02$ L mol^{-1} and $I_0 = 1.327$. As previously in the case of DPFA[19] we find an excellent agreement between the calculated and experimental values. This agreement gives evidence for the reaction network of Figure 1; in particular it indicates that DFFA does not form linear dimers or higher associates to an observable extent within the concentration and temperature range covered.

The values of K_{A_2} could also be determined from the analysis of the chemical shifts of ν_{A_a} of the mobile protons as well as of the fluorine atoms ν_{A_e,A_f} of the s-trans form as a function of the s-trans concentration C_A. The latter was calculated from the total concentration C and the value of I by using eq 46. The values of K_{A_2} were obtained by least-squares fitting of the experimental data to eq 54. At 194.5 K we obtained $K_{A_2} = 1.04$ L mol^{-1}, from the ^{19}F data (not shown) the value $K_{A_2} = 0.98$ L mol^{-1}. Thus, the values of K_{A_2} obtained by the different methods coincide within the margin of error. No detectable dependence of K_{A_2} on the deuterium fraction D in the mobile proton sites could be detected within the error limits.

The temperature dependence of K_{A_2} was determined exclusively by the analysis of the proton chemical shifts ν_{A_a}. From the van't Hoff plot we obtained the reaction entropy and enthalpy

$$\Delta S_{A_2} = -29 \pm 1 \text{ J mol}^{-1} \text{ K}^{-1},$$
$$\Delta H_{A_2} = 5.7 \pm 0.3 \text{ kJ mol}^{-1}, \quad 170 \text{ K} < T < 254 \text{ K} \quad (59)$$

(b) Kinetics of the s-Trans/s-Cis Isomerism. The pseudo-first-order rate constants k_{AB} of the s-trans/s-cis isomerism were determined by ^{19}F line-shape analysis in the high-temperature region as shown in Figure 5. In particular, samples with $C = 0.02$ mol L^{-1} and 0.35 mol L^{-1} were analyzed. No kinetic H/D isotope effect on the rate constants could be determined. According to eq 48, using the known values of I/I_0 the k_{AB} values could be converted into the first-order rate constants $k_{A_1B_1}$. The data are described by the equation

$$k_{A_1B_1} = 10^{14.3\pm1} \exp[(-62.5 \pm 1 \text{ kJ mol}^{-1})/RT] \text{ s}^{-1},$$
$$237 \text{ K} < T < 302 \text{ K} \quad (60)$$

(c) ^1H NMR Proton Inventory of DFFA in THF. The result of the measurements shown in Figure 3 are analyzed in Figure 9, where we have plotted the ratio of the inverse proton lifetimes in A $\equiv$ AH, $\tau_{AHA^*H}^{-1}(D)/\tau_{AHA^*H}^{-1}(D=0) = \tau_{AH}^{-1}(D)/\tau_{AH}^{-1}(D=0)$ as a function of D. We observe a linear decrease, as predicted by eq 57 for a double proton transfer process with $m = 2$. The inverse lifetimes $\tau_{AH}^{-1}(D=0)$ and $\tau_{AH}^{-1}(D=1)$ can then be identified as the pseudo-first-order rate constants k^{HH} and k^{HD} defined in eqs 14–19. By linear regression analysis we obtained $k^{HH} = 700 \pm 20$ s^{-1} and $k^{HD} = 37 \pm 5$ s^{-1}, i.e., a kinetic HH/HD isotope effect of $k^{HH}/k^{HD} = 19 \pm 3$. The relatively large error of the latter quantity is explained by the fact that we were not able to measure τ_{AH} values at $D > 0.9$ in this study by ^1H NMR spectroscopy.

(d) Rate Law of the Proton Exchange and the Kinetic HH/HD/DD Isotope Effects. Once the pseudo-first-order rate con-

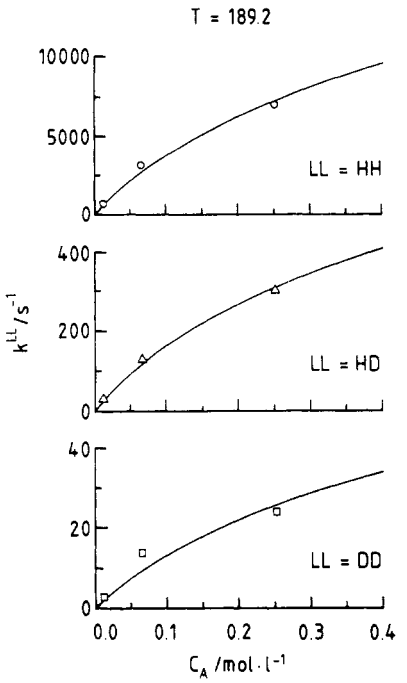

Figure 10. Nonlinear least-squares fit of the kinetic data obtained in the experiments shown in Figure 6 at 189.2 K at different values of D. For the calculations a fixed value of K_{A_2} = 1.12 L mol^{-1} was used.

stants k^{LL}, LL = HH, HD, DD, were determined either by lineshape or by magnetization transfer experiments, the true rate constants $k_{A_2}^{LL}$ of the double hydrogen transfer in the cyclic dimers were determined as shown previously for DPFA.[19] Either the k^{HH} values were plotted as a function of $(I - I_0)/(I + I_0)$, which gave linear relations as predicted by eq 56. From the slope of these curves the rate constants $k_{A_2}^{HH}$ of exchange in the dimer could be obtained. Another way was to plot the k^{HH} values as a function of C_A. At low C_A values the curves obtained are linear in C_A; at higher concentrations k^{HH} levels off and becomes independent of C_A as predicted by eq 55. Using the known values of K_{A_2}, we obtained the k_{A_2} values. Both methods were found to be in good agreement.

In the next stage we checked that the rate law does not depend on the deuterium fraction D. This is the case as shown in Figure 10 where the data of Figure 6 have been analyzed. The solid curves in Figure 10 were obtained by nonlinear least-squares fitting using the same known value of K_{A_2} at 189.2 K. Thus, within the margin of error there are no equilibrium isotope effects on the dimerization process. From the analysis in Figure 10 we obtained the rate constants $k_{A_2}^{HH}$ = 42 000 s^{-1}, $k_{A_2}^{HD}$ = 1990 s^{-1}, and $k_{A_2}^{DD}$ = 190 s^{-1} of the exchange in the cyclic dimers. All the results are assembled in Table 6 (supplementary material). The corresponding Arrhenius diagram is shown in Figure 11. The data can be represented by

$$k_{A_2}^{HH} = 10^{9.9\pm0.3} \exp[(-18.9 \pm 0.3 \text{ kJ mol}^{-1})/RT] \text{ s}^{-1} \quad (61)$$

$$k_{A_2}^{HD} = 10^{10.7\pm0.3} \exp[(-26.7 \pm 0.3 \text{ kJ mol}^{-1})/RT] \text{ s}^{-1} \quad (62)$$

$$k_{A_2}^{DD} = 10^{11.5\pm0.3} \exp[(-33.4 \pm 0.3 \text{ kJ mol}^{-1})/RT] \text{ s}^{-1} \quad (63)$$

$$164.2 \text{ K} < T < 260.9 \text{ K}$$

with the isotope effects at 189.2 K of

$$k_{A_2}^{HH}/k_{A_2}^{HD} = 23 \pm 4, \quad k_{A_2}^{HD}/k_{A_2}^{DD} = 10 \pm 2, \quad k_{A_2}^{HH}/k_{A_2}^{HD} = 237 \pm 20 \quad (64)$$

The error limits are of purely statistical origin and do not include possible systematic errors.

Discussion

From the results presented in the previous section it can be concluded that diarylamidines such as DPFA and DFFA are subject in tetrahydrofuran to the reaction network of Figure 1. This network could be characterized in a quantitative way. Especially the kinetic HH/HD/DD isotope effects were measured in a wide temperature range. The main part of this discussion is devoted to the mechanism of the double proton transfer emerging from these results.

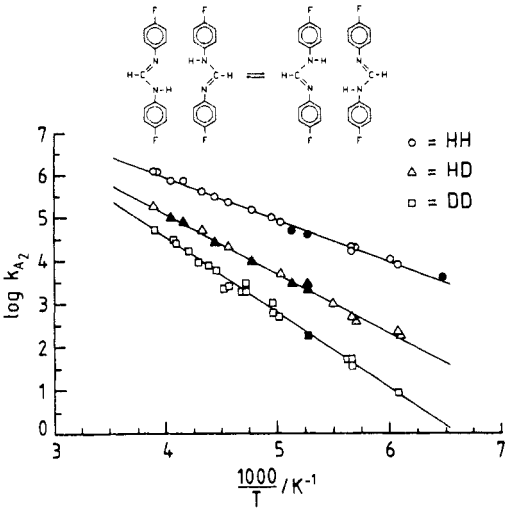

Figure 11. Arrhenius diagram of the HH, HD, and the DD transfers in cyclic s-trans dimers of DFFA dissolved in THF. The filled symbols were derived from sets of samples with different concentrations, the open symbols from single samples.

Reaction Network of Diarylamidines in THF. (a) s-Trans/s-Cis Isomerism. At low concentrations both DFFA conformers A and B are present as quasi-monomers A_1 and B_1 (Figure 1). Free monomers are present only in a very small concentration. A_1 has approximatively the same free energy as B_1 in the whole temperature range as found previously already for the related DPFA.[19] The rate constants $k_{A_1B_1}$ (eq 60) are relatively small, the energy of activation being 62.5 kJ mol^{-1} for DFFA and 59.7 kJ mol^{-1} for DPFA.[19] The frequency factors ($10^{14.3}$ and $10^{13.8}$ s^{-1}) are typical values for unimolecular reactions. No dependence of the isomerism on the deuterium fraction in the mobile proton sites could be observed.

(b) Self-Association of the s-Trans Conformer. Since hydrogen bond exchange between different hydrogen-bonded species is, generally, extremely fast on the NMR time scale, association phenomena of proton donors can be monitored by observing their chemical shift changes as a function of concentration. In the case of DFFA only the line positions of the s-trans form A of DPFA shift to lower field when concentration is increased but not of the s-cis form. This observation signifies that only the s-trans conformer A dimerizes to an observable extent in THF. From the analysis of the chemical shifts and the s-trans/s-cis ratio the equilibrium constants K_{A_2} of the formation of the A_2 dimer could be obtained in a wide temperature range. For DPFA a reaction enthalpy of −4.8 kJ/mol and for DFFA of −5.7 kJ/mol was found. The entropy decrease upon dimerization is −21.6 J/mol K for DFFA and −29 J/mol K for DPFA. No dependence of the isomerism on the deuterium fraction in the mobile proton sites could be observed.

The finding that only the s-trans form A dimerizes in THF to an observable extent but not the s-cis form B is plausible in view of the chemical structure of both conformers. By contrast to B, A can easily form a cyclic dimer with two cooperative hydrogen bonds. A consequence of the different association behavior is that the s-trans form is favored over the s-cis form when concentration is increased.

This interpretation is supported by the results of a recent crystallographic study of DPFA in the solid state.[44] In that study it was shown that DPFA forms cyclic dimers in the solid state

(44) Anulewicz, R.; Krygowski, T. M.; Pniewska, B. *J. Cryst. Spect. Res.* **1987**, *17*, 661.

with an intermolecular nitrogen–nitrogen distance of 2.98 Å. It is interesting to note that the four phenyl rings of each dimer are not equivalent. In the first molecule of the dimer the angles between the phenyl rings and the amidine plane are 59.3° and 9.7°; in the second molecule the angles are 30.7° and 37.7°. The angle between the two amidine planes is 40.6°. Note that the tendency to form cyclic dimers is much stronger for diarylamidines as compared for example to acetic acid. For the latter only evidence for linear solvated dimers in THF were obtained previously.[45]

(c) Double Proton Transfer in the Cyclic s-Trans Dimers. The fast proton transfer in the cyclic dimers is manifest in the spectral changes described in the previous section. As is demonstrated in Figures 3, 5, and 10 the proton exchange rates increase upon an increase of concentration. This enabled us to establish the rate law of the proton exchange (Figure 10). At low concentrations the pseudo-first-order constants increase linearly with concentration as expected for a second-order rate law involving two s-trans molecules of DFFA. At higher concentrations a nonlinear increase is observed as expected if the exchange takes place in the cyclic dimer. The nonlinear curve can be reproduced with the theory described in the Theoretical Section, which contains the equilibrium constant of the cyclic dimer formation K_{A_2} as parameter. Thus, the true exchange rates k_{A_2} in the cyclic dimer could be obtained, which is important when one wants to compare the kinetic results of the DFFA tautomerism with those of intramolecular double proton transfer reaction systems.

The number of protons transferred could be obtained independently by performing a proton inventory, i.e., by measuring the pseudo-first-order rate constants as a function of the deuterium fraction D in the mobile proton sites. We observed a linear decrease with D as expected for *two* protons transferred (eq 57, Figure 9). From these measurements we also obtained the kinetic HH/HD isotope effects of the exchange. To obtain the complete HH/HD/DD isotope effects, we performed ^{19}F NMR experiments on DFFA. In the ^{19}F spectra we observed the protonated and the deuterated molecules separately. Because of large kinetic isotope effects the DD rates were so small that they had to be determined by magnetization transfer experiments. These results show that the exchange in the cyclic dimer is the rate-limiting step of the reaction.

The experimental kinetic HH/HD/DD isotope effects on the double proton transfer in the cyclic dimer of DFFA, $k_{A_2}^{LL}$, LL = HH, HD, DD, are given by eqs 61–64. The data are shown in the Arrhenius diagram of Figure 11. At room temperature, the exchange in the cyclic A_2 dimers is about 4 times faster for DFFA as compared to DPFA.[19] The energies of activation of the exchange are similar, i.e., E_A^{HH}(DFFA) = 18.9 kJ mol^{-1} and E_A^{HH}(DPFA) = 17.2 kJ mol^{-1}.[19] The energies of activation of the HD reaction are E_A^{HD}(DPFA) = 21 kJ mol^{-1} and E_A^{HD}(DFFA) = 26.7 kJ mol^{-1} which show a larger difference. E_a^{DD}(DPFA) could not be obtained in the previous study.[19] By contrast, E_A^{DD}(DFFA) could be determined via ^{19}F NMR to be of the order of 33.4 kJ mol^{-1}.

The rate constants $k_{A_2}^{LL}$ of the tautomerism of DFFA dimers can directly be compared with those found for intramolecular reaction systems such as oxalamidines,[16,18] azophenine,[14] or porphyrins (Figure 12).[12] The tautomerism of the latter molecules is much slower as compared to DFFA dimers; this is mainly due to the fact that DFFA can form fairly linear hydrogen bonds, whereas the hydrogen bonds in the systems mentioned are bent bonds arising from constraints of the molecular backbone.

Kinetic HH/HD/DD Isotope Effects of Double Proton Transfer in Cyclic Diarylamidine Dimers. In this section we will discuss the size of the experimental kinetic HH/HD/DD isotope effects on the double proton transfer in the cyclic DFFA dimer and the mechanism which is consistent with these effects.

(a) Qualitative Discussion of the Kinetic HH/HD/DD Isotope Effects. As expressed by eq 63 we obtained the kinetic isotope effects $k_{A_2}^{HH}/k_{A_2}^{HD} \approx 23$, $k_{A_2}^{HD}/k_{A_2}^{DD} \approx 11$, $k_{A_2}^{HH}/k_{A_2}^{DD} \approx 237$ at 189.2 K. Clearly, these results signify that both hydrogen atoms are in flight in the rate-limiting step of the reaction. The same conclusion was reached previously for the double proton transfer in mixed 1:1 dimers of acetic acid and methanol dissolved in THF[12] where values of $k^{HH}/k^{HD} \approx 5$, $k^{HD}/k^{DD} \approx 3$, and $k^{HH}/k^{DD} \approx 15$ were found at 298 K (Figure 12d). Although the overall isotope effects are different, in part because of the differing temperature, one can conclude that both processes (Figure 12d,e) are characterized by two primary isotope effects.

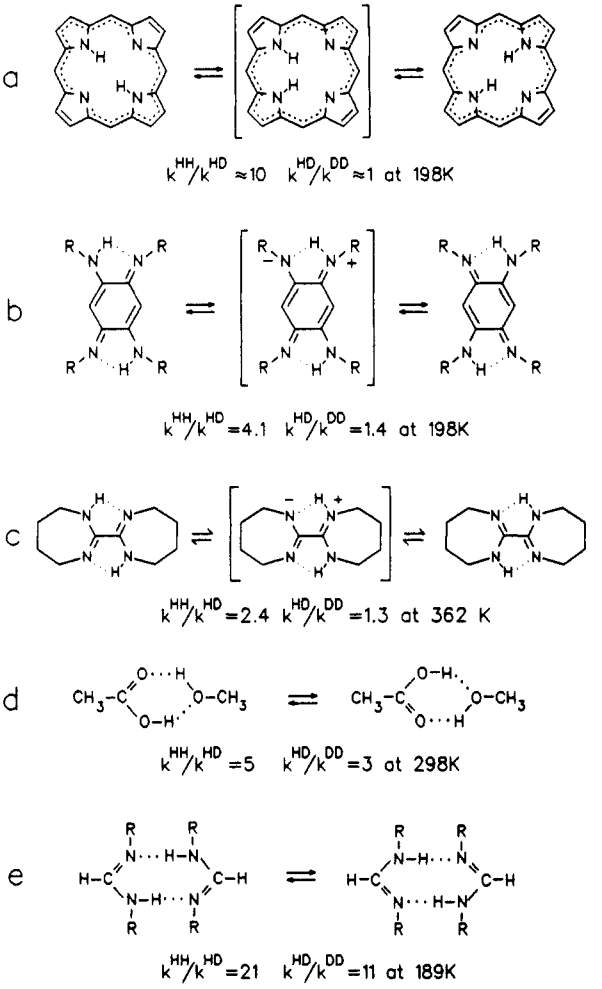

Figure 12. Kinetic HH/HD/DD isotope effects of some degenerate to intra- and intermolecular double proton transfer systems.

Rewriting eq 2 in the form

$$\frac{k^{HD}}{k^{DD}} = \frac{2}{P_1^{-1} + P_2^{-1}}, \quad \frac{k^{HH}}{k^{DD}} = P_1 P_2 \tag{65}$$

where P_1 and P_2 are now the kinetic isotope effects of the first and the second proton transferred, we calculated for the DFFA tautomerism using eqs 63 and 65 the values $P_1 = 37.3$ and $P_2 = 6.4$ at 189.2 K.

By contrast, as indicated in Figure 12, differing behavior was observed in the case of several degenerate intramolecular double proton transfer reactions. In these cases the kinetic HH/HD isotope effects were larger than 4 at 298 K, whereas the HD/DD isotope effects were in the order of 1–2. These results could be interpreted in terms of a stepwise double proton transfer involving a metastable intermediate where $P_1 \gg 1$ is a primary and $P_2 \simeq S \simeq 1$ a secondary isotope effect. In the case of DFFA P_2 is too large to be interpreted in terms of a secondary kinetic H/D isotope effect. Therefore, an explanation of the observed kinetic isotope effects for DFFA in terms of a simple stepwise proton transfer mechanism with fixed hydrogen bond distances as in the intramolecular cases seems to be unlikely.

(b) Calculation of the Arrhenius Curves in Terms of a Concerted Proton Motion. The calculation of the Arrhenius curves should,

(45) Gerritzen, D.; Limbach, H. H. *J. Phys. Chem.* **1980**, *84*, 799.

in principle, be done on the basis of a realistic ab initio surface using a theory of chemical reaction rates that takes multidimensional tunneling of protons into account. Such a calculation is difficult and beyond the scope of this study. Therefore, we apply here the one-dimensional Bell model[46] of proton tunneling that uses adjustable parameters. This model has, after a small modification, successfully been applied to the case of double proton transfer between acetic acid and methanol.[12,14] It has been shown that deviations from the rule of the geometric mean (RGM) can arise even in the case of a concerted double proton transfer if tunneling is involved.[13,14] As the Bell model, it uses an inverted parabola as an effective barrier. Effects of a distribution of different environments characterized by different microscopic potential energy surfaces[47,48] are ignored. By contrast to the Bell model, a minimum energy ΔE necessary for tunneling to occur is introduced.

We will assume here a concerted reaction pathway. Then, the RGM holds in the high-temperature region where the reaction proceeds over the barrier. Because of the concerted proton motion the tunneling masses are assumed to be $m = 2$, 3, and 4 for the HH, HD, and DD reaction.

Within the framework of this model the rate constant is given by

$$k = A\left\{\int_0^\infty G \exp[-E/RT]\, dE\right\} \Big/ \left\{\int_{-\Delta E}^\infty \exp[-E/RT]\, dE\right\} = (\nu/\mathrm{RT}) \exp[-\Delta E/RT] \int_0^\infty G \exp[-E/kT]\, dE \quad (66)$$

A is the frequency with which the particle hits the barrier; it is assumed to be the same for all isotopic reactions. R is the gas constant; E the energy. $E = 0$ corresponds to the base of the energy barrier. G is the probability of the particle to pass the barrier of height E_d at the energy E. G is given by[46]

$$G = 1/(1 + D) \quad (67)$$

where D is the transmission coefficient for a parabolic barrier of the width $2a$ and the height E_d:

$$D = \exp\left[-\left[\frac{2^{3/2}\pi^2}{h}(E_d - E)a(m/E_d)^{1/2}\right]\right] \quad (68)$$

E_d and a depend on the isotopic reaction studied and on the mechanism of the reaction. Let us first consider the barrier of the reaction. Defining $\Delta\epsilon^{LL}$ as the difference of the vibrational zero-point energies in the initial state and the transition state of the LL reaction, the effective barrier of the LL reaction is given by

$$E_d^{LL} = E_d + \Delta\epsilon^{LL} \quad (69)$$

For a concerted double proton transfer reaction the barrier for the HD reaction is assumed to be in approximation equal to the arithmetic means of the barrier for the HH and the DD reaction:

$$E_d^{HD} = \tfrac{1}{2}(E_d^{HH} - E_d^{DD}) \quad (70)$$

Thus, we can write

$$E_a^{DD} = E_a^{HH} + \Delta\epsilon = E_a^{HD} + \Delta\epsilon/2 \qquad \Delta\epsilon = \Delta\epsilon^{DD} - \Delta\epsilon^{HH} \quad (71)$$

The barrier width also depends on the isotopic reaction. For the parabolic barrier we obtained

$$a^{LL} = a^{HH}(E_d^{LL}/E_d^{HH})^{1/2} \quad (72)$$

To perform the tunnel calculations, a computer program was written in which the rate constants of all isotopic reactions could be fitted simultaneously to eq 66. As shown in Figure 13 we obtained a good fit using the following parameters: $\Delta E = 5.43$ kJ mol^{-1}, $E_d^{HH} = 26.2$ kJ mol^{-1}, $2a = 0.64$ Å, $A = 10^{12.5}$ s^{-1}, and $\Delta\epsilon = 5.89$ kJ mol^{-1}. These calculations postulate a strong curvature of the Arrhenius curves in a wide temperature range, barely perceptible in the temperature range covered.

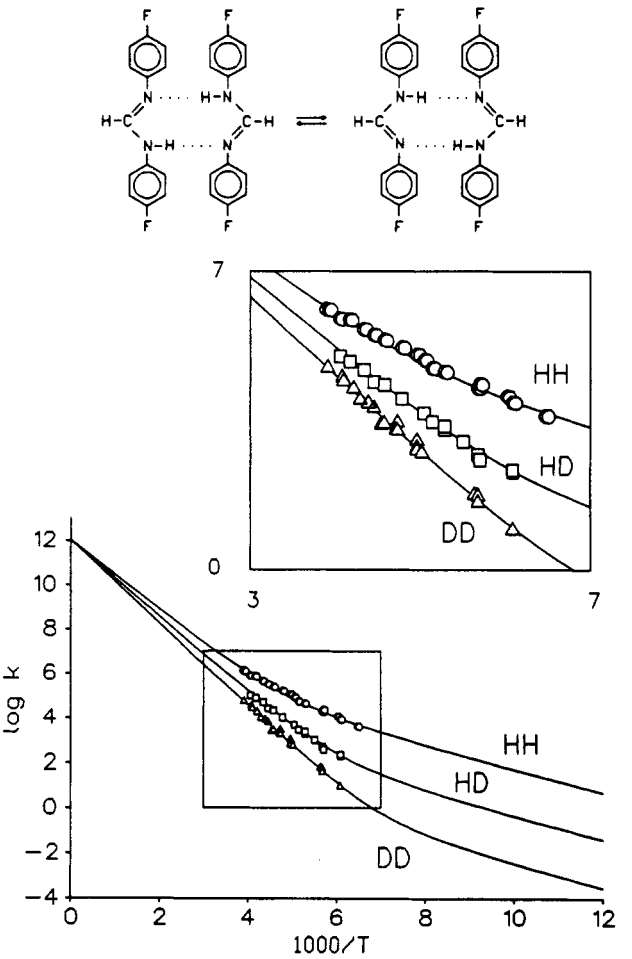

Figure 13. Comparison of the experimental rate constants of the HH, HD, and the DD transfers in cyclic s-trans dimers of DFFA in THF with those calculated in terms of the tunnel model described in the text.

In terms of this tunneling model it is interesting to extrapolate the kinetic isotope effects to 298 K. We obtained the values 14.3, 4.1, and 3.5 for the HH/DD, the HH/HD, and the HD/DD isotope effects. Because of the postulated curvature of the Arrhenius curves these effects are different from the values 8.2, 3.9, and 2.1, which we obtained by linear extrapolation from eqs 61–63 at $T = 298$ K. It is also interesting to calculate the classical kinetic HH/HD/DD isotope effects at 298 K for the reaction over the barrier from the relation

$$k^{HH}/k^{HD} = k^{HD}/k^{DD} = \exp(-\Delta\epsilon/2RT) \quad (73)$$

We obtained the values 11, 3.3, and 3.3 for the HH/DD, the HH/HD, and the HD/DD isotope effects. These values may be compared with those calculated by Ahlberg et al.[37] from a preliminary ab initio surface for the concerted double proton transfer in the unsubstituted formamidine dimers within the framework of transition state theory. These authors found the values 7.79, 2.76, and 2.82 for the HH/DD, HH/HD, and HD/DD isotope effects, which is consistent with a value of $\Delta\epsilon = 5.1$ kJ mol^{-1} and eq 73. In view of all approximations that have to be made and the fact that we have studied a formamidine derivative, the good agreement is surprising. At least, the magnitude of $\Delta\epsilon \approx 6$ kJ mol^{-1} found here by simulation of the Arrhenius curves seems to be in the right range.

The frequency factor of $A^{HH} \approx A^{HD} \approx A^{DD} \approx 10^{12.5}$ s^{-1} employed in the calculations of Figure 13 is also a good value for a unimolecular reaction. The sum of the minimum energy for tunneling to occur and the energy barrier $\Delta E + E_d^{HH} \approx 32$ kJ

(46) Bell, R. P. *The Tunnel Effect in Chemistry*; Chapman and Hall: London, 1980.
(47) Wehrle, B.; Zimmermann, H.; Limbach, H. H. *J. Am. Chem. Soc.* **1988**, *110*, 7014.
(48) Wehrle, B.; Limbach, H. H. *Chem. Phys.* **1989**, *136*, 223.

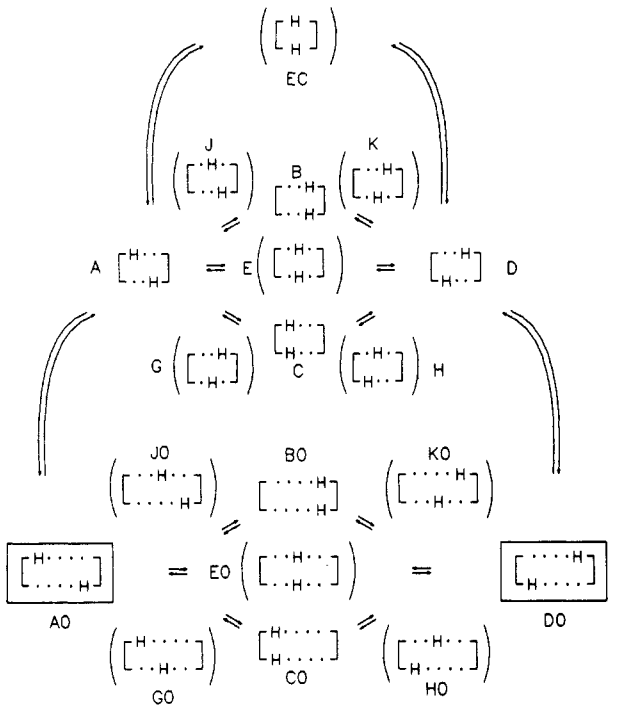

Figure 14. Reaction pathways of an intermolecular degenerate double proton transfer reaction.

mol^{-1} determines the slope of the HH–Arrhenius curve at high temperatures. This value also corresponds well with the value of 38 kJ mol^{-1} calculated by Ahlberg et al.[37]

What is the significance of the value of the minimum energy $\Delta E \simeq 5$ kJ mol^{-1} necessary for tunneling to occur? A priori we would have expected ΔE to be close to zero because the rate constants k_{A_2} measured refer to the double proton transfer in the cyclic dimer. Thus, these values should not contain terms arising from the preequilibrium $2A_1 \rightleftharpoons A_2$, by contrast to the previous study of proton exchange between acetic acid and methanol.[14] A possible source for ΔE is that the actual potential curves along which the protons are transferred are not symmetric as in the gas phase but slightly asymmetric on average because of intermolecular interactions, in a time scale of slow molecular motion. ΔE corresponds then to an effective energy difference of the two stable potential wells. Such perturbations of potential energy curves of proton transfers have been recently observed by solid-state NMR for proton transfer systems in disordered solid environments.[47,48] Other sources for ΔE might be the processes of equalizing the two CN bond lengths and the reorientation of the aryl groups in DFFA. If the proton motion is stepwise as discussed in the next section, ΔE might also arise from the formation of the metastable intermediate during the course of the reaction. Minimum energy is necessary to reach this intermediate. Finally, ΔE might arise from the fact that the model assumed is too simple in order to describe a very complex process.

The remaining quantity to discuss is the value of the barrier width $2a = 0.64$ Å. How does this value relate to the geometry of DFFA? Since a crystal structure analysis of DFFA has not yet been made to our knowledge, let us refer to the structure of DPFA,[44] where an NH distance of $R^{\circ}_{NH} \approx 1.1$ Å and an NN distance of $R^{\circ}_{N\cdots N} \approx 3$ Å was found. Thus, the experimental proton transport distance should be $2a^{cryst} \approx R_{N\cdots N} - 2R^{\circ}_{NH} \approx 0.8$ Å, which reproduces surprisingly well the value obtained from Figure 13.

Simplified Model of Degenerate Intermolecular Double Proton Transfer. The evidence for the concerted reaction pathway of double proton transfer in cyclic DFFA dimers is, in contrast to the previous evidence, that degenerate intramolecular double proton transfer reactions between nitrogen atoms (Figure 12) are stepwise. Such a change of mechanisms is, however, not the main difference one expects a priori for intra- and intermolecular double proton transfer systems. The expected difference is the following.

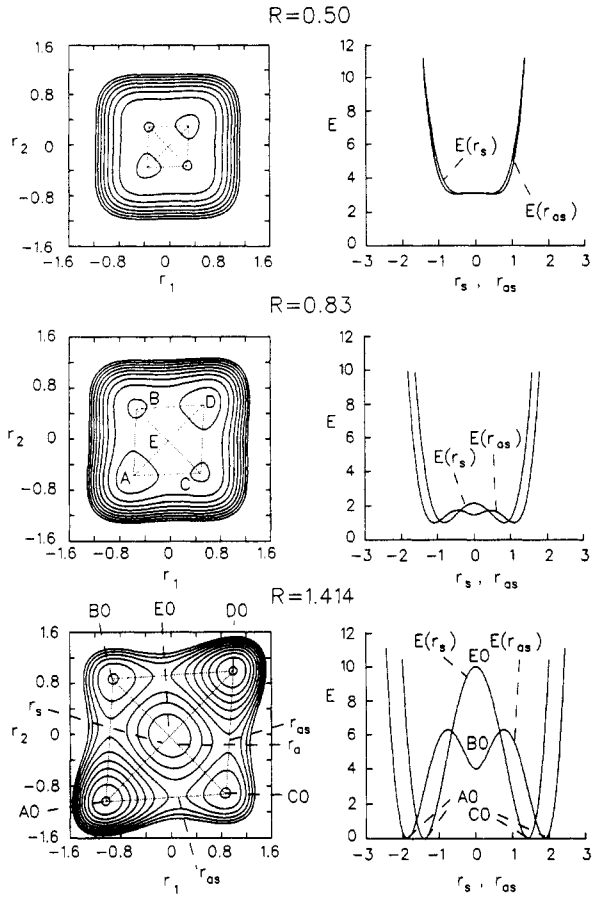

Figure 15. Model potential energy surface for a degenerate intermolecular double proton transfer, with $E_{A0} = 0$, $E_{E0} = 10$, $E_{B0} = 4$, $EC = 6$, $R_0 = 2^{1/2}$. r_1, r_2 are the coordinates of the two protons, R is the coordinate of the heavy-atom motion as defined in the text. r_s, r_a, and r_{as} are represented by dotted lines. r_s, r_a, and r_{as} represent the coordinates of the transfer A → E → D, B → E → C, and A → B → D or A → C → D. Left-hand side: bottom, $E_{min} = 0.1$, maximum contour line $E_{max} = 9.1$, energy difference between two lines $\Delta E = 1$; middle, $E_{min} = 2.58$, $E_{max} = 9.58$, $\Delta E = 1$; top, $E_{min} = 1.6$, $E_{max} = 9.6$, $\Delta E = 1$.

In contrast to intramolecular proton transfer systems intermolecular proton transfer systems are characterized by a low-frequency ($\sim$100 cm^{-1}) hydrogen bond stretching vibration.[49] Due to anharmonic coupling, compression of the hydrogen bond should strongly reduce the barrier for proton transfer.[14,49] There is experimental evidence in the case of 7-azaindole that excitation of the symmetric hydrogen bond stretch promotes the proton tautomerism in this compound.[11] The different structures that may lie on the reaction pathway are shown in Figure 14. The bottom reaction network corresponds to the ground-state geometry with equilibrium hydrogen bond lengths. Depending on the basicity of the heavy atoms to which the protons are bound, the proton transfer pathway in this configuration is either concerted or stepwise. The intramolecular systems of Figure 12 indicate that in many NH···N proton transfer systems the stepwise route is realized. Upon compression of the hydrogen bonds the reactants may become so close that eventually the barrier for proton transfer vanishes, i.e., the proton moves in a single-minimum potential. The following question then arises: *Can the compression of the hydrogen bond lead to a switch from a stepwise reaction mechanism to a mechanism where both protons are in flight*?

To explore this question, we used a symmetric three-dimensional model potential surface of the type $E = E(r_1,r_2,R)$ described in the Appendix. The variables are r_1 and r_2 for the motion of the two protons and R for the heavy atoms. The surface depends on the parameters R_0, E_{A0}, E_{B0}, E_{E0}, and E_{EC}. R_0 is the heavy-atom

(49) *The Hydrogen Bond*, Schuster, P., Zundel, G., Sandorfy, C., Eds.; North Holland: Amsterdam, 1976.

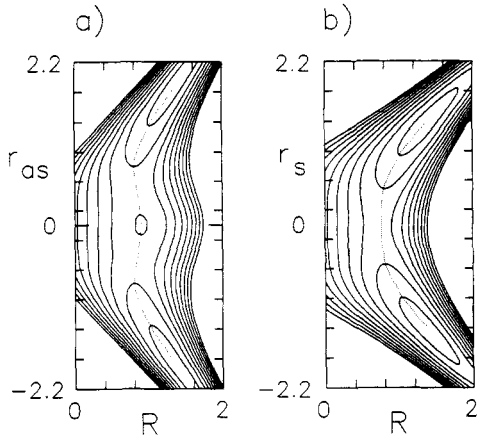

Figure 16. Two-dimensional potential surfaces (a) $E(R,r_{as})$ and (b) $E(R,r_s)$. $E_{min} = 0.5$, $E_{max} = 9.5$, $\Delta E = 1$.

distance in the ground-state configuration. E_{A0}, E_{B0}, E_{E0}, and E_{EC} represent the energies of the states defined in Figure 14. Examples with $R_0 = 2^{1/2}$, $E_{E0} = 10$, $E_{EC} = 6$, and $E_A = 4$ are shown on the left-hand side of in Figure 15, for different values of R. Clearly, the state E0 (see Figure 14) corresponds to a hilltop rather than to a saddle point as calculated for the porphyrin[50] and the azophenine[51] tautomerism. The minimum energy pathway corresponds to the coordinate r_{as} of the stepwise motion via the minima B0 and C0. When R is decreased, the energy differences between the points A, B, and E are drastically reduced and the protons move in a flat potential. It is interesting to discuss the reaction energy profiles along the concerted pathway ($E = E(r_s,r_a = 0)$) and the stepwise pathway ($E = E(r_{as})$). The coordinates r_s, r_a, and r_{as} are defined in the Appendix and are illustrated in Figure 15 by dotted lines. The profiles were calculated as indicated in the Appendix and are plotted on the right-hand sides of Figure 15. For $R = R_0$ the barrier energy $E_{E0} - E_{A0} = E^{\ddagger}_s(R)$ for the synchronous pathway is much larger than the corresponding energy $E^{\ddagger}_{as}(R)$ for the stepwise pathway. For smaller R values the profiles along the two pathways coincide. As R decreases, both $E^{\ddagger}_s(R)$ and $E^{\ddagger}_{as}(R)$ go through a minimum that can easily be calculated. For the parameters used in Figure 15 we obtain the following results. The true barrier for the stepwise motion is obtained at $R_m = 0.825$. The barrier has dropped from a value of about 6 at $R = 2^{1/2}$ to a value of $E^{\ddagger}_{as}(R_m) = 1.771$. The barrier for the synchronous motion has also dropped from a value of 10 at $R = 2^{1/2}$ to the minimum value $E^{\ddagger}_s(R_m) = 2.11$ at $R_m = 0.834$. Thus, whereas the stepwise pathway is preferred at large hydrogen bond lengths, both pathways compete when the hydrogen bonds are compressed.

Finally, it is interesting to discuss the surfaces $E = E(R,r_{as})$ and $E = E(R,r_s,r_a=0)$ for the stepwise and the concerted proton motion shown in Figure 16. The minimum energy reaction pathways are indicated by dotted lines. In the case of the stepwise motion there is a true intermediate that corresponds to states B and C in Figure 15. The reaction starts with a heavy atom motion mainly along the R axis. The protons can tunnel vertically at different R values or move over the barrier along the minimum energy pathway.

Mechanism of the Amidine Tautomerism. Unfortunately, it is not yet possible to calculate the kinetic HH/HD/DD isotope effects by combining the potential surface proposed in the previous section with the Bell model of tunneling. Qualitatively, we expect that tunneling along both the stepwise and the synchronous pathway might contribute to the reaction rates, which complicates the calculation of the kinetic isotope effects. In addition, we expect that even in the case of the stepwise motion the bound proton will contribute substantially to the kinetic isotope effects because its vibrational frequency is strongly reduced in the transition states G, H, J, and K in Figure 14 by contrast to G0, H0, J0, and F0. Therefore, the secondary isotope effect contributed by the bound proton will increase and eventually become a primary kinetic isotope effect, depending on the exact location of the true transition state. Thus, the experimental kinetic isotope effects are in agreement not only with a concerted proton transfer involving tunneling but also with a stepwise pathway which first involves the compression of the hydrogen bonds.

(50) Merz, K. M.; Reynolds, C. H., *J. Chem. Soc., Chem. Commun.* **1988**, 90.

(51) Holloway, K. M.; Reynolds, C. H.; Merz, K. M. *J. Am. Chem. Soc.* **1989**, *111*, 3466.

Conclusions

We have described the rate constants and kinetic HH/HD/DD isotope effects of a degenerate intermolecular double proton transfer reaction, i.e., the tautomerism of a cyclic formamidine dimer (DFFA) has been obtained as a function of temperature by dynamic NMR spectroscopy. Each proton contributes a primary kinetic hydrogen/deuterium isotope effect to the reaction rates, by contrast to several intramolecular double proton transfer systems where the second proton only contributes a secondary isotope effect because the reaction is stepwise involving a metastable intermediate. There is evidence for a more or less concerted reaction mechanism for the DFFA tautomerism, involving tunneling at low temperatures. The different behavior of the intra- and intermolecular reaction systems is attributed to the relatively low energy necessary to compress the hydrogen bond length in the intermolecular reaction systems. In the highly compressed systems the difference between the concerted and the stepwise proton transfer mechanism disappears.

In the future, it will be desirable to study the amidine tautomerism also in the solid state and to perform ab initio calculations of the isotopic rate constants.

Acknowledgment. We thank the Deutsche Forschungsgemeinschaft, Bonn–Bad Godesberg, and the Fonds der Chemischen Industrie Frankfurt for financial support. The calculations were done on the Univac 1108 computer of the Rechenzentrum der Universität Freiburg i.Br.

Appendix

Extending the usual symmetric double minimum potential to two extensions we obtain

$$E = E_E - \frac{E_E - E_A}{R^2}r_s^2 + \frac{1}{R^2}[(E_E - E_A)(E_E - E_B)]^{1/2}r_a^2 + \frac{3}{4R^2}(2E_E - E_A - E_B)[(E_E - E_A)/(E_E - E_B)]^{1/2}r_a^2r_s^2 + \frac{E_E - E_A}{4R^4}(r_s^4 + r_a^4) \quad (A1)$$

$E_A = E_D$, $E_B = E_C$, and E_E are the energies of the states A, D, B, C, and E defined in Figure 14. The variables r_s and r_a are given by

$$r_s = (1/2^{1/2})(r_1 + r_2), \quad r_a = (1/2^{1/2})(r_1 - r_2) \quad (A2)$$

r_1 and r_2 are the displacements of the protons from the hydrogen bond centers. For $r_a = 0$, r_s represents the coordinate of the concerted proton motion along the pathway A → E → D. r_a represents the concerted proton motion along the pathway B → E → C. When a double proton transfer occurs between states A and D each proton travels from $r_1 = r_2 = -R$ to $r_1 = r_2 = R$. Thus, R characterizes the increase of the hydrogen bond length with respect to the compressed state EC in Figure 14. Assuming that

$$E_E = E_{E0}\frac{R^4}{R_0^4} + E_{EC}\left(\frac{R}{R_0} - 1\right)^2$$

$$E_A = E_{EC}\left(\frac{R}{R_0} - 1\right)^2 \quad (A3)$$

$$E_B = E_{B0}\frac{R^4}{R_0^4} + E_{EC}\left(\frac{R}{R_0} - 1\right)^2$$

we obtain using eqs A1 and A2 a three-dimensional surface of the type $E = E(r_1,r_2,R)$ depending on the parameters R_0, E_{A0}, E_{B0}, E_{E0}, and E_{EC}. Equation A1-A3 are valid only for the case where $E_E > E_B$.

The reaction energy along the stepwise pathway ($E = E(r_{as})$) is given by

$$E = E_E - \frac{E_E - E_A}{R^2} b^2 r_{as}^2 + \frac{(E_E - E_B)}{R^2}(r_{as}b + 2^{1/2}R)^2 + \frac{3(2E_E - E_A - E_B)}{4R^4} b^2 r_{as}^2 (r_{as}b + 2^{1/2}R)^2 + \frac{E_E - E_A}{4R^4} r_{as}^4 + \frac{E_E - E_B}{4R^4}(r_{as}b + 2^{1/2}R)^4,$$

$$b = [\{1 + [(E_E - E_B)/(E_E - E_A)]^{1/2}\}^{1/2}]^{-1} \quad \text{(A4)}$$

For a given R value the barrier of the stepwise motion is located at

$$r^{\ddagger}_s = -\frac{R}{8}\frac{(8E_{E0} - E_{A0} - 7E_{B0})}{2E_{E0} - E_{A0} - E_{B0}},$$

$$r^{\ddagger}_a = -\frac{R}{8}\left[\frac{E_{E0} - E_{B0}}{E_{E0} - E_{A0}}\right]^{1/4}\frac{(8E_{E0} - 7E_{A0} - E_{B0})}{2E_{E0} - E_{A0} - E_{B0}} \quad \text{(A5)}$$

For the energy $E^{\ddagger}_{as}(R)$ of the saddle point along the stepwise pathway we obtain

$$E^{\ddagger}_{as}(R) = E_{EC}\left(\frac{R}{R_0} - 1\right)^2 + \frac{R^4}{R_0^4}\left[E_{E0} - E_{A0} - 2(E_{EO} - E_{A0})\frac{r_s^2}{R_0^2} - 2(E_{E0} - E_{B0})\frac{r_a^2}{R_0^2} + 3(2E_{E0} - E_{A0} - E_{B0})\frac{r_s^2 r_a^2}{R_0^4} + (E_{E0} - E_{A0})\frac{r_s^4}{R_0^4} + (E_{E0} - E_{B0})\frac{r_a^4}{R_0^4}\right] \quad \text{(A6)}$$

The minimum of $E^{\ddagger}_{as}(R)$ is located at

$$R_m = R_0\left[\left\{\frac{a}{2} + \left[\left(\frac{a}{2}\right)^3 + \left(\frac{a}{2}\right)^2\right]^{1/3}\right\}^{1/3} - \left\{-\frac{a}{2} + \left[\left(\frac{a}{2}\right)^3 + \left(\frac{a}{2}\right)^2\right]^{1/3}\right\}^{1/3}\right], \quad a = E_{EC}/2A \quad \text{(A7)}$$

$E^{\ddagger}_{as}(R_m)$ is the true barrier for the stepwise motion. The corresponding value for the concerted proton motion $E^{\ddagger}_s(R_m)$ is obtained by setting

$$a = E_{EC}/(2(E_{E0} - E_A)) \quad \text{(A8)}$$

in eq A7.

Registry No. DFFA, 18464-36-3; D_2, 7782-39-0.

Supplementary Material Available: Tables 1-6 containing all numerical data obtained by data analysis of the NMR experiments described in this study (7 pages). Ordering information is given on any current masthead page.

Deprotonation Energy and Charge Redistribution in Excited States of Acetylene†

Vijaya Marudarajan and Steve Scheiner*

Department of Chemistry and Biochemistry, Southern Illinois University, Carbondale, Illinois 62901
(Received: March 8, 1991)

UHF and UMP3 level calculations with a 6-31+G** basis set are used to investigate the ground and first few excited electronic states of HCCH and its deprotonated anion, HCC^-. All excited states are found to adopt a bent geometry, some cis and some trans in the case of HCCH. The deprotonation energies of these excited states do not differ much from that of the ground state. The bending of the molecule leads to a transfer of electron density from C to H when an electron is deposited into the lower π^* virtual MO. This trend is surprisingly invariant with respect to the particular excited state.

Introduction

The transfer of a proton from one group to another underlies all of acid/base chemistry.[1,2] Within the regime of biology, such transfers are vital to the functioning of a number of enzymes.[3-5] Photon-induced proton transfers have been shown to be a viable means of inducing lasing activity.[6-10] The first step in the latter process involves the electronic excitation of a molecule containing a hydrogen bond. The properties of the H-bonding groups are altered within the excited state such that a proton transfer occurs rapidly and exoergically. The subsequent relaxation to the ground state sets the stage for the reverse transfer of the proton back to the original configuration.

A large body of work has accumulated over the years concerning hydrogen bonding and proton transfers within the ground electronic state.[1,2,11,12] Recent ab initio computations[13-20] have outlined the importance of such features as the relative proton affinities of the two groups, their distance of separation, and the angular aspects of their relative geometry. In comparison, very little is clearly understood about the parallel transfer in the excited state. In any case, it is certainly reasonable to expect the proton affinities of the various groups in their excited states to play a crucial role in proton transfers between them in the corresponding state. For

† Dedicated to Professor Michael Kasha on the occasion of his 70th birthday.

(1) Bartmess, J. E.; McIver, R. T., Jr. In *Gas Phase Ion Chemistry*; Bowers, M. T., Ed.; Academic Press: New York, 1979; Vol. 2, Chapter 11.
(2) Caldin, E. F.; Gold, V. *Proton-Transfer Reactions*; Wiley: New York, 1975.
(3) Silverman, D. N.; Lindskog, S. *Acc. Chem. Res.* **1988**, *21*, 30.
(4) Cho, Y.-K.; Cook, P. F. *Biochemistry*, **1989**, *28*, 4155.
(5) Craik, C. S.; Roczniak, S.; Largman, C.; Rutter, W. J. *Science*, **1987**, *237*, 909.
(6) Parthenopoulos, D. A.; Kasha, M. *Chem. Phys. Lett.* **1988**, *146*, 77.
(7) Kasha, M. *Acta Phys. Pol.* **1987**, *A71*, 717.
(8) Chou, P.; McMorrow, D.; Aartsma, T. J.; Kasha, M. *J. Phys. Chem.* **1984**, *88*, 4596.
(9) Barbara, P. F.; Walsh, P. K.; Brus, L. E. *J. Phys. Chem.* **1989**, *93*, 29.
(10) Itoh, M.; Hasegawa, K.; Fujiwara, Y. *J. Am. Chem. Soc.* **1986**, *108*, 5853.
(11) *The Hydrogen Bond. Recent Developments in Theory and Experiments*; Schuster, P., Zundel, G., Sandorfy, C., Eds.; North-Holland: Amsterdam, 1976.
(12) *Hydrogen Bonds*; Boschke, F. L., Ed.; Springer-Verlag: Berlin, 1984.
(13) Bosch, E.; Lluch, J. M.; Bertran, J. *J. Am. Chem. Soc.* **1990**, *112*, 3868.
(14) Cao, H. Z.; Allavena, M.; Tapia, O.; Evleth, E. M. *J. Phys. Chem.* **1985**, *89*, 1581.
(15) Brciz, A.; Karpfen, A.; Lischka, H.; Schuster, P. *Chem. Phys.* **1984**, *89*, 337.

0022-3654/91/2095-10280$02.50/0